# Characterization of V3 Interneuron Firing Patterns During Rhythmic Locomotor-Like Ventral Root Activity

by

Rachele Molyneaux

A thesis submitted to the

Faculty of Graduate Studies and Postdoctoral Studies

of the University of Manitoba

In partial fulfillment of the requirements of the degree of

**Master Of Science**

Department of Physiology and Pathophysiology

Max Rady College of Medicine

Rady Faculty of Health Sciences

University of Manitoba

Winnipeg, MB

**Abstract**

V3 interneurons (INs) are a genetically defined population of glutamatergic spinal neurons implicated in regulating the robustness of locomotion. Previous studies using computational modeling have postulated that V3 INs play a critical role in maintaining robust, coordinated alternation during rhythmic motor output. However, to date, no studies have directly recorded from identified V3 INs during rhythmic locomotor-like activity in the mammalian spinal cord. Therefore, the purpose of this study is to characterize the intrinsic electrophysiological properties and activity patterns of V3 INs during rhythmic motor activity using whole-cell patch-clamp (WCPC) recordings in Sim1Cre/TdTomato P1–P5 mouse spinal cord preparations. Electrophysiological recordings were preformed prior to and during pharmacologically induced tonic and rhythmic locomotor like ventral root (VR) activity via perfusion of serotonin (5-HT) and N-methyl-D-aspartate (NMDA). Analysis to date indicate that most V3 INs are quiescent at baseline, although some demonstrate spontaneous activity. Variable responses were recorded from V3 INs during drug evoked tonic VR activity. Specifically, following 5-HT and NMDA application and the emergence of tonic VR activity, most V3 INs recorded to date displayed an increase in excitability. This was characterized by a depolarized resting membrane potential and an increased firing rate correlating with the onset of tonic activity in VR recordings. Conversely, some V3 INs demonstrated decreased activity during drug evoked tonic VR activity, suggesting functional diversity within the recorded V3 INs. Similarly, V3 INs recorded during rhythmic VR activity also appeared to be tonic. However, due to our limited sample size, future research should aim to examine a larger sample and record V3s in a wider range of spinal segments to determine whether the observed pattern of firing during drug evoked locomotor activity is a more widespread phenomena/characteristic. These findings will provide critical insights into the cellular mechanisms and contributions of V3 INs to the generation and modulation of spinal locomotor circuits.

## Acknowledgments

I would like to express my sincere gratitude to my advisor, **Dr. Jeremy Chopek**, for his support and guidance throughout the course of this project. His confidence in me as a student has played an insurmountable role in shaping both this thesis and my development as a researcher. I am also deeply thankful to my co-advisor, **Dr. Kris Cowley**, for her thoughtful feedback, expertise, and continued support during all stages of this work.

I would like to thank my committee members, **Dr. Micheal Jackson** and **Dr. Brent Fedirchuk**, for their valuable input, critical discussions, and constructive feedback, which greatly strengthened my thesis and critical thinking skills.

Special thanks are extended to **Narjes**, whose technical expertise, dedication, and assistance during experimental procedures were essential to the successful completion of this work.

I am incredibly grateful to my mentors and friends**, Dr. Lucia** and **soon-to-be Dr. Camila**, whose support extended far beyond the laboratory. Thank you for always knowing when a coffee break, led day, or moment of laughter was needed; your friendship made this journey far more enjoyable.

I would also like to thank my family for encouraging me to return to school and pursue a field that truly inspired and challenged me. Their unwavering support, both in and out of the lab, provided the foundation that made this achievement possible.

Finally, I am deeply thankful to my friends **Ashley, Elyssa, Dana, Justine, Ayo, Haily and Julia,** for always having my back. Thank you for ensuring I always had a night out (or in) when you knew I needed it; your support, phone calls, laughter, and understanding carried me through even the most demanding moments.

I would also like to acknowledge the members of the **Spinal Cord Research Centre (SCRC)** for fostering a collaborative and supportive research environment, with particular thanks to **Katinka Stecina** for her kindness and support.

And last but not least, I would like to thank my dog, **Millie**, for being an unconditional companion throughout this journey (with the exception of moments when someone else was holding a treat).

This work would not have been possible without the guidance, encouragement, and support of all those mentioned above.

# Table of Contents

## List of Tables

## List of Figures

## List of Abbreviations

**CPG:** central pattern generator

**CIN:** commissural interneuron

**IN:** interneuron

**MLR:** mesencephalic locomotor region

**RF:** reticular formation

**EAA:** excitatory amino acid

**NMDA**: n-methyl-d-aspartate

**NMA:** n-methyl-aspartate

**PIC:** persistent inward current

**CNS:** central nervous system

**DTA:** diphtheria toxin a

**RGN:** rhythm generating network

**5-HT:** serotonin

**DA:** Dopamine

**aCSF:** artificial cerebral spinal fluid

**raCSF:** ringer artificial cerebral spinal fluid

**VR:** ventral root

**CC:** central canal

**FF:** firing frequency

$\mathbf{R_{in}}$: resistance input

**RMP:** resting membrane potential

**HCN:** hyperpolarization-activated cyclic nucleotide-gated

**PIR:** post-inhibitory rebound

# Chapter I: Introduction

## 1.1 Historical Foundation of Locomotor Control

Locomotion is a trait which is deeply embedded in human evolution and is fundamental to human survival (Fu et al., 2019). Vertebrate locomotion (e.g., swimming, walking, trotting) is produced by coordinated, rhythmic activation of spinal motor networks and their peripheral effectors (Ijspeert, 2003). A fundamentally integral and regulatory aspect of locomotion, which allows for the rhythmic generation of musculoskeletal movements, are reflexes. Reflexes incorporate various neurological mechanisms that are essential for rapid motor responses and environmental integrations. Facilitated by neural synapses within the spinal cord through a 'reflex arc', these circuits permit rapid activation of spinal motor neurons without supraspinal processing (Derderian et al., 2023).

### 1.1.1 Polysynaptic Reflexes Implicated in Rhythm Generation

The ability to activate these circuits, independent of the brain, was first discovered in 1906, when Sir Charles Sherrington demonstrated that initiation of the scratch-reflex in dogs with transected spinal cords could evoke a rhythmic pattern of hind limb movement through reciprocal inhibition, intrinsic to the spinal cord (Rybak et al., 2015). Sherrington later evaluated the crossed-extension reflex, a reflex that resulted in the lift and forward swing of one leg which was accompanied by a converse action on the other leg that supports this movement. He discovered that, when given a tonic stimulus, the spinal cord was able to produce a *successive coordination* (Sherrington, 1910) during spinal stepping. These observations were later supported with more advance techniques that allowed for intracellular recording of motoneuronal activity during stimulation of flexor reflex afferents (Jankowska et al., 1967). While reflex arcs exemplify the spinal cord's remarkable capacity for rapid and adaptive responses to sensory

stimuli, they represent just a fraction of its intricate neural circuitry. However, these findings were essential in developing the foundational concept of motor control and locomotion used in Brown's research on the spinal central pattern generator (CPG) (Brown, 1911, 1914).

### 1.1.2 Central Pattern Generators

Building on these foundational observations of polysynaptic reflex organization, early 20th-century work demonstrated that spinal circuits could coordinate flexor and extensor motor output through distributed interneuronal networks. First proposed by Brown in 1914, the locomotor CPG model challenged the prevailing reflex-chain theory of locomotion (Brown, 1914; Sherrington, 1910) by suggesting the spinal cord could generate rhythmic locomotor activity intrinsically – without requiring phasic sensory feedback or descending cortical input. Brown introduced the concept of the "half center" oscillator, consisting of two ipsilateral groups of spinal INs on each side of the body: one group of INs responsible for flexor activity and the other group of INs responsible for extensor activity. These two groups were thought to reciprocally inhibit each other, giving rise to the flexor-extensor oscillation commonly observed during principal rhythmic motor behaviours such as walking or swimming (Brown, 1914). Brown proposed the principal of *progressive augmentation* as the key mechanism behind the oscillatory ability of the two half-centers meaning that when one half-center is active, it exerts a strong inhibitory influence on the opposing center to reinforce its own activity. However, over time, the active half center experiences fatigue, leading to a decline in its activity and a release of inhibition on the opposing center. This allows for the previously inhibited center to become active, resulting in a phase switch and continuation of the rhythmic cycle. Brown's half-center model thus provided an intrinsic mechanistic model for both rhythmogenesis (self-sustained rhythm generation) and phase switching (flexor–extensor alternation) in locomotion. However,

its simplified structure failed to capture the complexities of real locomotor behaviours, such as a delayed transition from stance to swing phase when the limb experiences an increased load, as observed in biological systems (Conway et al., 1987).

During locomotion, some motor pools remain functionally isolated as either flexor or extensor, while others contribute to both types of contractions (L. A. Cohen & Cohen, 1956; Rossignol & Terjung, 1996). This supports the observations of mixed-synergy motor patterns such as paw shake (Carter & Smith, 1986) and the stumbling corrective reaction (Forssberg, 1979), where muscles are recruited outside of their typical flexor-extensor roles. Brown's classical half-center model, which assumed a strict alteration between flexor and extensor activity, cannot account for the functional flexibility observed in these findings. Consequently, subsequent research shifted toward identifying the biological mechanisms that enable the complexity and adaptability of real locomotor behaviors.

Engberg and Lundberg postulated a role for proprioceptive feedback in mediating extensor-flexor activity; proposing that sensory afferents coordinate extensor-flexor transition during more complex tasks and adjust gait based on changes in load, terrain or speed (Engberg & Lundberg, 1969). This idea was further supported by Grillner and Rossignol (1977) and Duysens *et al.* (1980), who examined the effects of hip and ankle positioning on the initiation and/or continuation of locomotion in the cat, respectively. They demonstrated that these key proprioceptive signalling pathways are crucial for interlimb coordination and gait transition. Notably, proprioceptive feedback can delay the onset of gait transition from flexion to extension during treadmill walking when a large load is applied, as this activates Ib afferents which in turn inhibit the subsequent flexion (Duysens & Pearson, 1980). Later studies showed that, during fictive locomotion, excitation of ipsilateral extensor group Ib afferents could reset the locomotor

pattern on the contralateral limb (Conway et al., 1987). This highlights the critical role that afferent feedback plays, particularly from load receptors, in shaping the timing and activation of the locomotor CPG.

### 1.1.3 Intrinsic Organization and Mechanisms of the Spinal Locomotor CPG

While sensory feedback is crucial for modulating ongoing locomotor patterns, intrinsic spinal mechanisms also contribute to the complexity and adaptability of the spinal locomotor CPG. In 1981, Grillner proposed the idea that the spinal locomotor CPG is composed of modular "unit burst generators" that are thought to underlie the production of specific muscle synergies (Grillner, 1981). Located along the rostral caudal axis of the spinal cord and near the motoneurons they activate, these units are responsible for activating groups of closed synergistic muscle groups acting on a given joint (Cowley & Schmidt, 1997). Building upon this idea, significant work on the spatial distribution of these units uncovered differences in rhythmogenic capacity across spinal cord segments, with the rostral lumbar and caudal cervical being capable for producing hindlimb and forelimb locomotion, respectively (Cowley & Schmidt, 1997; Kiehn & Kjauerulff, 1998; Kjaerulff & Kiehn, 1996; Kremer & Lev-Tov, 1997). Moreover, the thoracic segments are thought to play a prominent role in intersegmental coordination and rhythm propagation, whereas lumbar and cervical segments are more directly involved in shaping limb-related motor patterns and extensor–flexor alternation.

These findings, along with others (Akay et al., 2014; Cowley & Schmidt, 1995; Kiehn, 2006, 2016) have shaped the modern understanding of the spinal locomotor CPG as a dynamic and spatially diverse network of INs capable of integrating intrinsic rhythmogenic mechanisms with supraspinal and sensory inputs over multiple segmental levels. Featuring two functionally distinct but interconnected layers: a rhythm-generating layer where basic locomotor rhythm is

generated, and a pattern formation layer where motor output across multiple joints and limbs is coordinated (McCrea & Rybak, 2008). This hierarchical organization allows for the flexible modulation and adaptation observed in daily movement that were lacking in Browns original single layer model **(Figure 1)**.

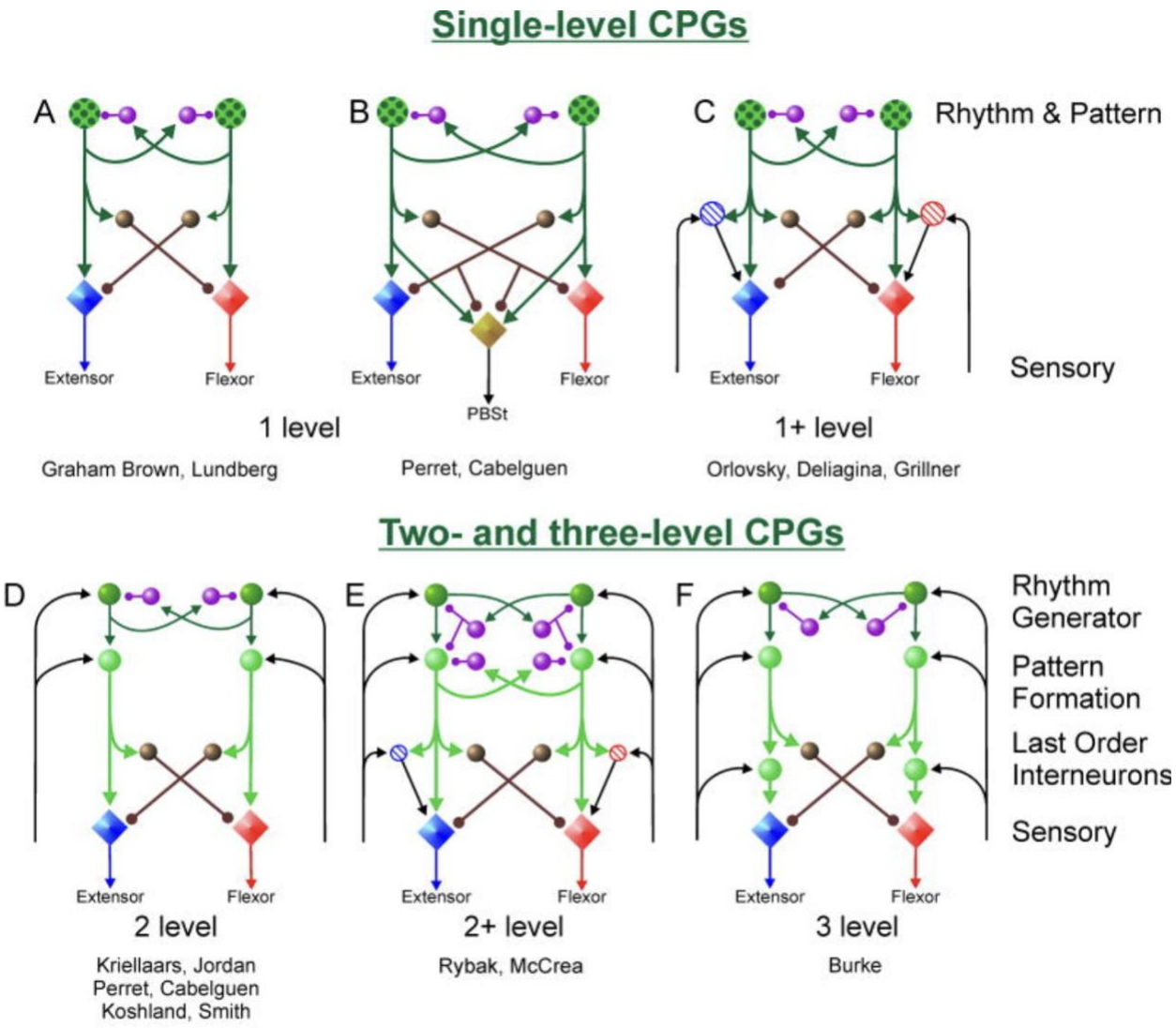


**Figure 1.** The organizational evolution of the spinal locomotor CPG (McCrea & Rybak, 2008). Excitatory synapses are characterized by arrow heads, while inhibitory are characterized by circles. In the single level CPGs, excitatory INs (green stippled INs) provide direct input to MNs. (A) is Browns classic half-center scheme. Two and three level CPG is associated with a rhythm generator (dark green) and a pattern formation network (light green). For this paper, we consider D-F "two-level" schemes. Reproduced from McCrea and Rybak, 2008, Fig 1.

### 1.1.4 Locomotor-Related Spinal INs

The layered organization of rhythm generation and pattern formation within the spinal locomotor CPG is supported by distinct classes of spinal INs that coordinate to produce and regulate locomotor output. Located in the ventral horn of the spinal cord, these neurons are positioned ideally to interact with motoneurons and modulate motor output directly (Kjaerulff & Kiehn, 1996). Based on their developmental origin from specific ventral progenitor domains, these neurons are classified into four principal cardinal classes: V0, V1, V2, and V3, with MNs begin the final output of the circuit **(Figure 2)**. Each class originates from distinct precursors that then gives rise to subpopulations of either excitatory or inhibitor neurons with diverse molecular identities, neurotransmitter phenotypes and projection patterns that may ascend, descend, or project ipsi- or contralaterally across the spinal midline. These developmental and physiological differences underlie their specialized roles in locomotor behaviour, such as left-right alteration, flexor-extensor timing and speed dependant gait modulation. A more detailed discussion of class-specific properties and phenotypes will be provided in Section 1.3.3.

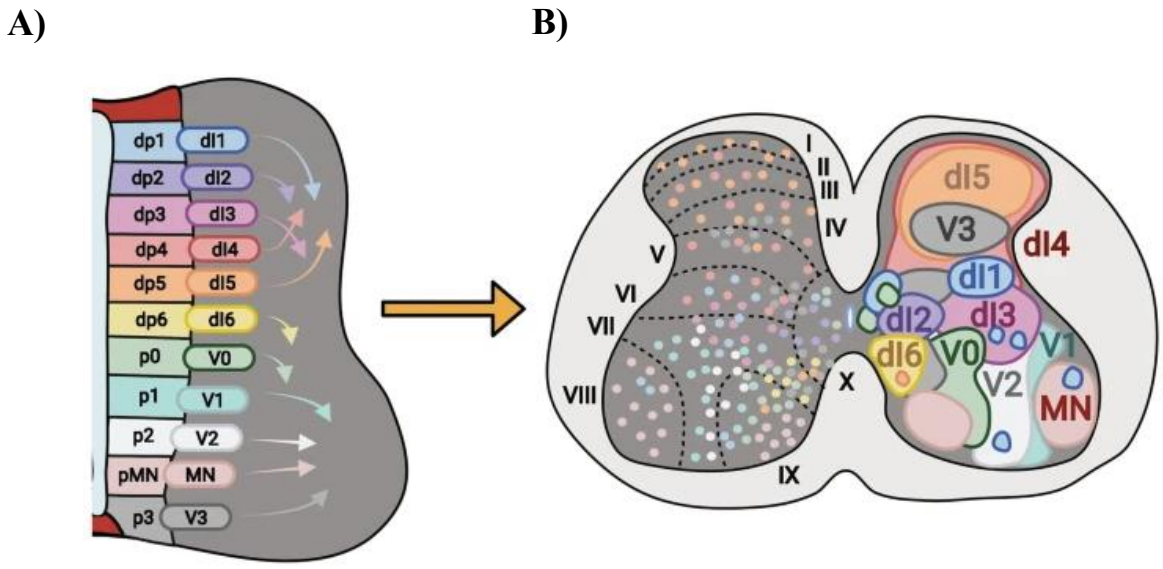

**Figure 2.** Development and settling patterns of spinal cord INs from the embryonic dorsoventral domains (a) to settling places within the adult spinal cord in relation to Rexed's lamina (b). Reproduced from (Matise & Rallo, 2022).

## 1.2 Experimental Approaches for Eliciting Locomotor-Like Rhythmic Activity

In neurologically intact animals, locomotion is initiated by activation of the mesencephalic locomotor region (MLR), which projects to and activates reticulospinal neurons within the reticular formation (RF). These descending pathways ultimately drive the spinal locomotor CPG responsible for coordinated and rhythmic locomotor activity. Early evidence for reflex-evoked locomotion came from studies in decerebrate dogs and cats, where cutaneous, noxious or proprioceptive afferent stimulation was shown to trigger stepping-like movements, even in the absence of supraspinal control (Brown, 1911; Sherrington, 1910). After which several different methods have been developed to study locomotion in both *in-vivo* and *in-vitro* preparations.

### 1.2.1 Locomotion Induction via Brain Stem Electrical Stimulation

In 1966, Shik, Severin and Orlovskii demonstrated that electrical stimulation of the posterior midbrain in decerebrate cats could reliably evoke locomotion, even in the absence of cortical input (Shik et al., 1966). They localized the effective stimulation area to the region comprising the pedunculopontine and cuneiform nucleus; now commonly known as the MLR. Importantly, they found that intensity of stimulation correlated with the speed of locomotion observed; lower intensity produced slow walking, while higher intensities induced faster gaits such as trotting or galloping. Later research revealed that stimulation of the descending tracts (McClellan & Grillner, 1984) and the pontomedullary RF play a role in the initiation and modulation of rhythmic locomotor-like activity (Jordan, 1998; Liu & Jordan, 2005).

This work was pivotal in establishing both the graded control of locomotor output by supraspinal centers, and the concept of top-down modulation of spinal locomotor networks, however, it also activated a broad range of descending pathways. These complexities made it difficult to isolate whether the resulting patterns originated from supraspinal commands or intrinsic spinal circuits. To address this limitation, researchers shifted toward a model of locomotion that was drug-induced, allowing for isolation of the spinal cord and eliminating supraspinal influence.

### 1.2.2 Locomotion Induction via Drug Application

The first clear evidence that neurochemicals alone could mimic natural descending glutamatergic input from supraspinal centers was shown through application of excitatory amino acids (EAAs), such as D-glutamate and catecholamine precursor L-DOPA to the isolated lamprey spinal cord (A. H. Cohen & Wallen, 1980; Poon, 1980). Bath application of these compounds reliably activated endogenous locomotor CPG networks, inducing sustained, rhythmic fictive locomotor patterns in the absence of descending input or sensory feedback. These early experiments provided strong evidence that the spinal cord contains an intrinsic rhythm-generating network, capable of producing coordinated motor output when provided with adequate excitatory drive.

Subsequent studies in the same preparation demonstrated that selective activation of N-Methyl-D-Aspartate (NMDA) receptors alone was sufficient to elicit rhythmic locomotor-like activity (Grillner et al., 1981). This was key in highlighting the critical role of NMDA receptors in generating and sustaining rhythmic oscillations in spinal INs. For example, in the isolated neonatal rat spinal cord, N-Methyl-D,L-aspartate (NMA) as well as NMDA were shown to reliably induce rhythmic motor output (Kudo & Yamada, 1987; Smith et al., 1988; Smith &

Feldman, 1985, 1987). These studies collectively emphasize the important role of NMDA receptors-mediated mechanisms in supporting sustained rhythmic activity of INs within the spinal locomotor CPG.

Since then, a wide range of neuromodulatory compounds have been used to evoke locomotor-like rhythmic activity via exogenous administration on the *in vitro* rat spinal cord, including kainate, dopamine, norepinephrine, acetylcholine, clonidine and other monoamines (Brodin et al., 1985; Cheng et al., 2019; Cowley & Schmidt, 1994; Forssberg & Grillner, 1973; Kiehn et al., 1992; Sharples et al., 2015). These compounds typically act by enhancing the excitability of spinal networks and facilitating activation of persistent inward currents (PICs) in motor- and INs.

Most notably, serotonin (5-HT) has proven particularly effective in facilitating PICS (Perrier & Delgado-Lezama, 2005) and modulating spinal excitability (Kudo & Yamada, 1987; Smith & Feldman, 1987; Viala & Buser, 1974). Many experiments confirmed that 5-HT, especially when co-applied with NMDA, significantly enhances the frequency, stability and coordination of locomotor-like rhythms (Barnes & Sharp, 1999; Cazalets et al., 1990, 1992; Cowley & Schmidt, 1994; Flaive et al., 2020). With subsequent studies indicating its superior ability to produce more robust and consistent (physiologically relevant) locomotor-like rhythmic behaviour than NMDA, dopamine or ACh alone (Kiehn & Kjaerulff, 1996). This has led to its routine use in rodent spinal cord preparations as a key neuromodulator to activate the spinal locomotor CPG.

### 1.3 Models for Studying Locomotion

The study of the spinal locomotor network has relied heavily on both *in vivo* and *in vitro* animal models. However, *in vitro* isolated spinal cord preparations have become essential for

investigating the neuronal network responsible for rhythm generation, coordination, and neuromodulatory control of locomotion as they offer accessible insight, stable and reproducible conditions, while maintaining physiological relevance. Over the past century, as scientific knowledge and technology have advanced, so too have the experimental techniques and model systems used to study these networks. From adult cats to primitive vertebrates and embryonic rodents, research on the core circuitry of locomotion has evolved, deepening our understanding of the neural basis of movement.

Early studies of the locomotor system were conducted in decerebrated or spinalized cats (Brown, 1911; Forssberg & Grillner, 1973). These adult mammalian models played a foundational role in establishing the concept of a locomotor CPG, as their size, robustness and physiological similarity to humans made them ideal for electrophysiological investigation (Duysens & Van de Crommert, 1998). However, the complexity of the adult mammalian CNS made it difficult, with technology available at the time, to dissect the detailed organization of these circuits. Consequently, researchers shifted toward simpler vertebrate models to enable more precise analysis of the fundamental components of the spinal locomotor CPG (A. H. Cohen & Wallen, 1980).

Among these, vertebrates such as the adult pleurodele, *Xenopus* embryo and tadpole, and mudpuppy have allowed for a detailed investigation of the operations of the spinal locomotor CPG involved in swimming and walking (Delvolvé et al., 1997; Frolich & Biewener, 1992; Roberts et al., 1998; Wheatley et al., 1992). However, the lamprey, a jawless and finless primitive vertebra, emerged as a simple model for studying the spinal circuitry involved in the rhythmic movement pattern of swimming (Grillner et al., 1981; Poon, 1980). With its relatively small quantity of cells and ancestral origin, the lamprey offers both simplicity and evolutionary

relevance, enabling research to investigate the foundations of vertebrate locomotion across approximately 500 million years of evolutionary history (Grillner & Jessell, 2009). Combined, these features have also made it one of the first systems in which dual intracellular recordings could be performed on pre- and postsynaptic INs and motoneurons, allowing for a detailed analysis of synaptic connectivity and rhythmic generating mechanisms (Buchanan & Grillner, 1987). Furthermore, its reduced complexity allowed for the genetic identification of different functional classes of INs populations contributing to the production of rhythmic motor activity (Buchanan, 2001; A. H. Cohen & Wallen, 1980; Poon, 1980), marking it as a key foundational model for studying basic principles of pattern generation, coordination and modulation in vertebrate systems.

The introduction of the isolated neonatal rat spinal cord in the 1980s provided the first reliable *in vitro* mammalian preparation for studying locomotor rhythms, which has since expanded to include neonatal and adult mouse models (Hernandez et al., 1991; Kudo & Yamada, 1987; Smith et al., 1988; Smith & Feldman, 1985, 1987; Tao & Droge, 1992). These preparations retain the capacity to generate and sustain rhythmic, locomotor-like activity when exposed to EAAs, cholinergic, and dopaminergic agonists, enabling stable ventral root recordings of motor output (Bonnot et al., 2002). Furthermore, the adaptability of rodent models has opened the door to advanced experimental techniques and genetic manipulations that allow researchers to activate locomotor circuity with note-worthy precision. This includes the use of optogenetics to manipulate specific neuronal populations (Falgairolle & O'Donovan, 2021; Hägglund et al., 2010), intracellular patch-clamp electrophysiological recordings to study intrinsic membrane properties and synaptic connectivity (Bakels & Kernell, 1993; Granit et al., 1963; Zagoraiou et al., 2009), and transgenic or knockout mouse lines that enable the

identification of genetically defined IN populations (Lanuza et al., 2004). For these reasons, combined with their accessibility, experimental feasibility, reproducibility, and compatibility with both pharmacological agents and genetic tools, these well-established rodent models have emerged as a useful tool for studying mammalian locomotor CPGs.

## 1.4 Techniques for Studying Locomotion

### 1.4.1 Electromyography (EMG) Recordings

The foundational techniques for EMG recordings were first partially established by Adrian and Bronk with the use of fine wire electrodes that were able to record motor unit action potentials in the rabbit (Adrian & Bronk, 1928). Since then, advancements in electrode design and signal amplification have greatly enhanced the ability to capture muscle reflexes, voluntary movement, and spinal circuitry output, (Engberg & Lundberg, 1969; Shik et al., 1966). As EMG technology evolved, it became an essential tool for probing the functional output of the spinal locomotor CPG. When combined with other techniques, such as intracellular recordings, EMG provides a boarder perspective on the structure and function of spinal motor circuits.

### 1.4.2 Ventral Root Recordings

Ventral root recordings are extracellular electrophysiological technique which are used to monitor motor output from the spinal cord during *in vivo* and *in vitro* locomotor studies. Small, glass suction electrodes are applied to the ventral roots which capture and record the compound action potentials generated by the motoneuronal populations (O'Donovan & Landmesser, 1987). These signals represent motor output of multiple motoneuronal populations innervating a specific group of muscles and provides a reliable approximate for the rhythmic motor output produced by the CPG. Commonly used alongside other methods such as EMG and intracellular recordings, ventral root or hindlimb electroneurogram recording allows for quantification of

variables such as step-cycle period, burst duration, phase relationship and intersegmental coordination (Cowley& Schmidt, 1997; Gosgnach et al., 2006; Kudo & Yamada, 1987).

### 1.4.3 Intracellular and Patch-Clamp Recordings

The highly technical intracellular electrophysiological recording techniques used today were first used in the 1950s by Sir John Eccles, who is best known for using sharp microelectrodes to study spinal motoneurons and INs in anesthetized cats (Brock et al., 1952; Eccles et al., 1954). These sharp electrodes marked the first wave of single-cell electrophysiology, providing direct access to membrane potentials and enabling researchers to experimentally test the ionic theory of synaptic transmission. Using this approach, Eccles and colleagues characterized synaptic events in detail, including the ionic mechanisms underlying EPSPs and IPSPs, particularly in the context of spinal reflex circuits and recurrent inhibition. Around the same time, Hodgkin and Huxley employed a similar intracellular approach in the squid giant axon to develop their quantitative model of action potential generation, establishing the biophysical principles of voltage-gated ion conductance (Hodgkin & Huxley, 1952). Together, these advances demonstrated that intracellular recordings could link cellular physiology with circuit-level function.

Although technically demanding, intracellular recordings were critical because they allowed investigators to directly measure synaptic potentials, inhibitory mechanisms, and motor firing properties; features that later became central to understanding how spinal circuits generate and regulate rhythmic motor output. Subsequent researchers further expanded upon these foundational concepts, including Elzbieta Jankowska, whose foundational work helped reveal the organization of reflex pathways and synaptic integrations of group I muscle afferents and spinal circuits (Jankowska et al., 1967), mapping functionally organized pathways and developing a

foundational understanding of the integration of sensory input at the spinal level and its integral role in modulating locomotion. And, over a decade later, Anders Lundberg, who used similar techniques to explore multisensory integration and descending control of spinal reflexes (Lundberg, 1979), and whose contributions have been extensively reviewed and contextualized (Hultborn, 2006).

By the early 1980s, limitations of sharp microelectrodes prompted the development of recording methods with improved stability, signal isolation, and the ability to resolve subthreshold membrane properties and ionic currents. The development of the patch-clamp technique in 1981 by Neher and Sakmann was a significant advancement. The introduction of the patch-clamp technique by Neher and Sakmann (1981) provided a major advance, as the high-resistance gigaseal enabled low-noise recordings from single channels and allowed precise voltage control of either the whole cell or a defined membrane patch (Hamill et al., 1981). The increased resolution and stability of patch-clamp electrophysiology subsequently enabled detailed characterization of intrinsic conductances and synaptic mechanisms, thereby linking cellular biophysics to the circuit-level processes involved in spinal rhythm generation.

### 1.4.4 Transgenic and Knockout Models

The development and use of transgenic and knockout models have allowed for a targeted approach of studying the organization and function of the spinal locomotor networks. By enabling the selective silencing, activation or ablation of neurons and based on their genetic identity, these models allow researchers to link individual IN populations to specific locomotor phenotypes, such as rhythmogenesis, interlimb coordination, and dynamic gait transition (Goulding, 2009b; Kiehn, 2016; Picciotto & Wickman, 1998). Central to these strategies is the identification of molecularly defined progenitor domains within the ventral neural tube, which

give rise to specific classes of INs. Each ventral neural progenitor domain (p0-p3 and pMN) is characterized by specific transcription factors, which modulate and guide the development of spinal ventral INs (Jessell, 2000). These transcription factors include Dbx1 (p0), En1 (p1), Chx10 (p2) and Sim1 (p3), and are responsible for the differentiation of V0-V3 locomotor-related INs, respectively (Briscoe et al., 2000; Goulding, 2009b; Lanuza et al., 2004; Zhang et al., 2008). It is with the identification of these class-specific transcription factors that has enabled targeted genetic labelling and manipulation (Deska-Gauthier & Zhang, 2019).

Techniques such as Cre-lox recombination, intersectional genetics and reporter lines rely on transcription factors to drive the expression of Cre-lox recombinase in defined neuronal populations. For example, a Dbx1:Cre knock-in mouse line, which uses floxed diphtheria toxin a (DTA) in Dbx1+ cells, creates a targeted ablation of the V0 INs early in development, demonstrating the critical function V0s have in coordinating contralateral motor outputs (Lanuza et al., 2004). In contrast, the Cre-lox system can also be utilized to permanently label genetically defined populations without altering their function. The $Sim1^{Cre}$; $R26^{floxstop\text{-}lacZ}$ reporter line was developed to visualize the developmental pattern and record the physiological properties of Sim1+ expressing V3 INs (Zhang et al., 2008).

**1.5 Locomotor Related INs**

Together, the application of transgenic and knockout models has transformed our understanding of locomotor-related INs from earlier, broad classifications such as flexor- and extensor-related interneurons (Jankowska et al., 1967) to detailed, genetically defined populations with discrete contributions to rhythm generation and interlimb coordination as described below. By combining transcription factor–driven genetic targeting with tools such as Cre-lox recombination and reporter lines, researchers have been able to move beyond identifying where

these neurons are located to defining what they do in the locomotor circuit. These approaches established links between genetically defined IN populations and specific locomotor phenotypes, revealing both shared and class-specific contributions to coordination, rhythm generation, and gait control.

### 1.5.1 V0 INs

V0s arise from the progenitor domain P0 and subdivided into ventral (V0v) and dorsal ($V0_D$) populations. They include both excitatory and inhibitory commissural INs (CIN) with distinct electrophysiological properties. There are additionally two ipsilaterally projecting V0s; $V0_C$ (cholinergic) and $V0_G$ (glutamatergic) classes make up approximately 2% of the total population, with the $V0_C$s playing a role in regulating the gain of high-output motor activity (Deska-Gauthier & Zhang, 2019). The V0s expresses the transcription factor Dbx1, while only $V0_V$s additionally express $Evx^1$ (Lanuza et al., 2004). Together, these neurons are further divided into subpopulations that contribute to backwards locomotion, scratching, righting and postural corrections (Zelenin et al., 2021).

### 1.5.2 V1 INs

V1 INs are Engrailed-1 (En1)–expressing inhibitory neurons that play a central role in shaping locomotor output. These ipsilaterally projecting INs arise from the progenitor domain P1 and form a heterogeneous population that includes classical Ia inhibitory INs, which mediate reciprocal inhibition of antagonist motoneurons. Renshaw cells are additionally derived from V1 INs, which provide recurrent inhibition to motoneurons (Gosgnach et al., 2006). Through these circuits, V1 neurons contribute to the fine-tuning of burst durations and coordination within the step cycle. Importantly, their influence on locomotor frequency is context-dependent: V1 activity has differential effects depending on the method used to evoke locomotion, as well as if the output

is flexor- or extensor-biased, highlighting their role in adapting the rhythm to the biomechanical and environmental demands of movement (Falgairolle & O'Donovan, 2021).

### 1.5.3 V2 INs

V2 INs arise from the progenitor domain P2 to mature into ipsilaterally projecting INs that express the TF Lhx3. They can be further divided into distinct V2a, V2b and V2c subclasses. Although originating from the same progenitor domain within the neural tube, V2 INs perform distinct tasks in the context of locomotion. V2a neurons are excitatory ipsilateral projecting INs defined by the expression of the transcription factor Chx10. Whereas V2b/c INs are inhibitory and defined by expression of the transcription factors Gata2/3 and $Sox1^{+}$ respectively. V2b INs play a primary role in establishing the alternating flexor–extensor rhythm, both in the presence and absence of V1 INs (Sengupta & Bagnall, 2022; J. Zhang et al., 2014) via reciprocal inhibition of V1s and V2as. They project ipsilaterally with descending axons and display rhythmic activity in phase (**Figure 3** depicts an example of a neuron that fires in-phase with VR activity) with the swim cycle during zebrafish locomotion, slightly preceding each ipsilateral motor burst (Sengupta & Bagnall, 2022).

$V2_a$ neurons, in mice, can be further subdivided into type I and type II populations, distinguished by their intra vs supraspinal projection patterns, differential regulation of the transcription factor Chx10 and by their expression of Shox2 (Hayashi et al., 2018; Rybak et al., 2015). Functionally, V2a type I INs support left–right alternation during mid-speed gaits, such as trotting, by providing excitatory rostral-caudal drive to V0v commissural pathways (Dougherty, 2023), while V2a type II INs are thought to operate at the PF level of the CPG, mediating rhythm-generating inputs to ipsilateral MNs and thus contributing to movement amplitude (Menelaou & McLean, 2019).

Most Chx10-expressing INs also express Shox2, although a smaller subset (approximately 25%) expresses *only* Shox2; known as Shox2$^{+}$ nonV2a INs (SnV2a). These SnV2a INs are rhythmically active during fictive locomotion and provide flexor-related input to motor neurons (Dougherty et al., 2013a; Rancic & Gosgnach, 2021). Silencing of SnV2a INs results in a reduction in locomotor frequency, supporting their role in CPG rhythmogenesis.

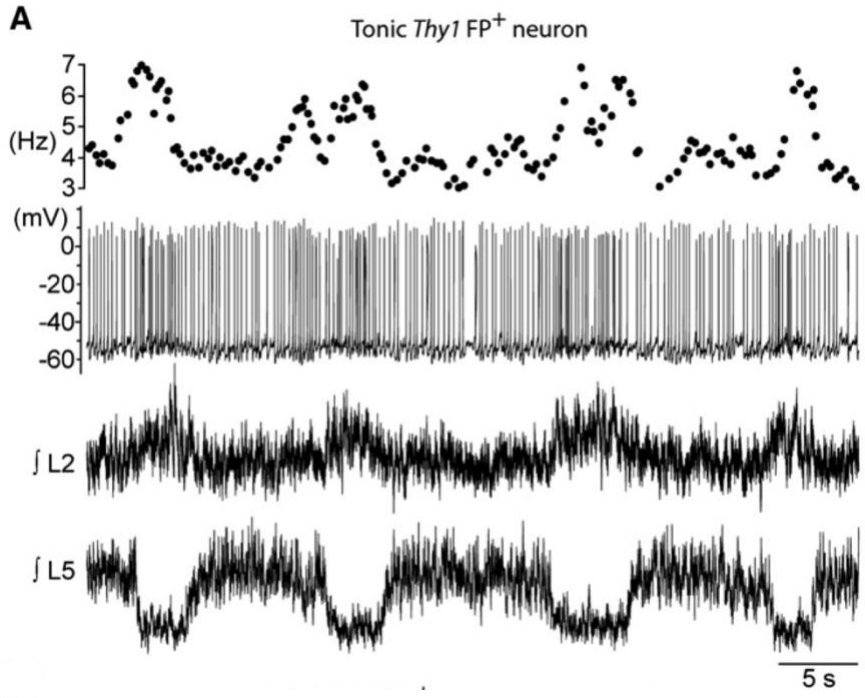


**Figure 3.** Current-clamp recording of a V0 neuron (top 2 traces) firing in phase with flexor related L2 ventral root and out of phase with extensor related L5 ventral root (bottom 2 traces) during drug induced fictive locomotion (Kiehn, 2016; McCrea & Rybak, 2008). Reproduced from Zagoraiou et al., 2009, Fig. 6A.

### 1.5.4 V3 INs

V3 neurons are excitatory CINs (Chopek et al., 2018a). They express the transcription factor single-minded 1 (sim1) and are distributed throughout lamina X, VIII, VII and deep dorsal horn of the spinal cord (Chacon et al., 2023; Cowley & Schmidt, 1997; Rancic & Gosgnach, 2021). Their projections are both ipsilateral and contralateral, with ascending and descending branches,

some reaching cervical levels, providing an anatomical basis for forelimb–hindlimb coordination (Blacklaws et al., 2015; Chacon et al., 2023).

During development, V3s segregate into ventral, dorsal and intermediate populations distinguished by their anatomical position, morphology, and electrophysiological properties (Borowska et al., 2013). Ventral V3s include medial V3s ($V3_{med}$) and lateral V3s ($V3_{lat}$) subtypes, where $V3_{med}$ INs synapse onto $V3_{lat}$ INs to distribute excitation to specific motor pools (Chopek et al., 2018a). They have been observed to directly synapse onto MNs, Renshaw cells, parvalbumin positive Ia inhibitory INs, and other V3 INs (Chopek et al., 2018b; Zhang et al., 2008).

Electrophysiologically, ventral V3s display properties of endogenous oscillators: they can rhythmically oscillate in the presence of NDMA, fire trains of action potentials, and therefore serve as effective distributors of excitation within the CPG (Borowska et al., 2015; Rancic & Gosgnach, 2021; Zhang et al., 2008). Dorsal, along with some intermediate V3s, primarily act as cutaneous afferents sensory relay INs with an important aspect in weight-bearing locomotion (Borowska et al., 2013). Collectively, V3s play a pivotal role in gait transitions and are thought to contribute to maintaining stable and robust locomotion (Chacon et al., 2023; H. Zhang et al., 2022).

Danner et al. (2019) introduced compelling evidence for ventral V3 INs being responsible for mutual excitation between left and right extensor centers of the rhythm generating network (Danner et al., 2019). These results indicate that V3 INs may play a predominant role in extension rather than flexion. A recent investigation examining the function of V3 INs during fictive locomotion in the larvae of zebrafish is the first empirical evidence of V3s being active during fictive locomotion (Wiggin et al., 2022). The results demonstrated V3 INs providing precisely timed, tonic excitatory drive to MNs to support swimming locomotive patterns in the zebrafish. Most notably, it was observed that when V3 INs were subjected to target ablation, there was a

significant (23.4%) reduction in the amount of MNs recruited to participate in locomotion, although the range of locomotor frequencies produced remained unaffected (Wiggin et al., 2022). Collectively, these findings suggest that V3s are more significantly implicated in the gain of motor control rather than the generation of rhythmic locomotor patterns.

### 1.5.5 HB9$^{+}$ INs

HB9$^{+}$ is a transcription factor expressed transiently in many ventral neurons during development; however, in the mature spinal cord it is maintained primarily in adult MNs and in a small subset of ventrally located interneurons in the caudal thoracic and rostral lumbar segments (T13–L2/3) (Hinckley et al., 2005) HB9$^{+}$ INs are ipsilaterally projecting, premotor glutamatergic neurons which are interconnected via electrical synapses and exhibit rhythmic activity during fictive locomotion (Dougherty & Ha, 2019). They are directly engaged by low-threshold afferents, and stimulation of this pathway during the flexion phase of the step cycle can reset the locomotor rhythm. This phase-dependent sensory reset closely parallels the electrophysiological behavior of ventral V2a (Chx10$^{+}$) interneurons, which are strongly recruited by group I/II low-threshold proprioceptive afferents and can reset or entrain locomotor output during flexion (Dougherty & Kiehn, 2010; McCrea & Rybak, 2008; Rybak et al., 2006; Zhong et al., 2010). Given their rhythmic, flexor-related activity, ventral positioning, and developmental proximity to V2a INs, HB9$^{+}$ INs may correspond functionally to this class of afferent-driven, rhythm-resetting premotor interneurons. Furthermore, their activity remains aligned with motor bursts, supporting a role for Hb9 INs in shaping the temporal structure of locomotor output (Dougherty & Ha, 2019; Hinckley et al., 2010). HB9+ INs are mutually and self-excitatory (Wilson et al., 2005), a characteristic seen in other rhythm-generating networks (RGN), with their activity being in-phase with rhythmic motor outputs.

## 1.6 Effects of Neurotransmitters on Locomotor Output

In isolated spinal cord preparations, rhythmic locomotor-like activity can be pharmacologically induced to study the intrinsic rhythmogenic mechanisms of the locomotor CPG. This is typically achieved using a combination of serotonin (5-HT), NMDA, and dopamine (DA) receptor agonists, which together modulate IN excitability and synaptic drive within spinal locomotor networks (Cazalets et al., 1990, 1992; Cowley & Schmidt, 1994; Hernandez et al., 1991). When applied individually, each neurotransmitter activates distinct components of the circuitry. Exogenously applied 5-HT is broadly understood to enhance the stability and coordination of locomotor rhythms, (Flaive et al., 2020), whereas NMDA primarily increases neuronal excitability (Wallen & Grillner, 1987), and dopamine modulates the overall excitatory tone (Sharples et al., 2015). However, when applied in combination, their effects are synergistic: 5-HT and NMDA jointly initiate stable rhythmic bursting, while dopamine refines and stabilizes the pattern, producing coordinated and robust locomotor output.

### 1.6.1 Serotonin (5-HT)

Serotonin (5-HT) was one of the first neurotransmitters shown to evoke fictive locomotion in spinalized rats (Cazalets et al., 1992; Cowley & Schmidt, 1994; Kiehn & Kjaerulff, 1996). Differential effects of exogenously applied 5-HT have been reported, however its broad effect is facilitating network activation by increasing burst stability and coordination. Acting primarily through $5\text{-HT}_{2A}$ and $5\text{-HT}_{7}$ receptors, 5-HT depolarizes INs by reducing $K^+$ leak currents and enhancing persistent $Na^+$ and $Ca^{2+}$ currents, thereby increasing neuronal excitability and rhythmic bursting when activated during the step cycle (Abbinanti & Harris-Warrick, 2012). In contrast, activation of the $5\text{-HT}_{1A}$ receptors can hyperpolarize inhibitory INs with, destabilizing fictive

locomotion, showcasing 5-HTs dual modulatory potential (Flaive et al., 2020; Schmidt & Jordan, 2000).

At the network level, 5-HT enhances coupling between rhythm-generating INs and strengthens left–right and flexor–extensor coordination within the locomotor pattern (Liu & Jordan, 2005). The effect of 5-HT on the frequency and amplitude of locomotor output is dose-dependent; low concentrations typically promote stable, slow rhythms, whereas high concentrations can lead to tonic or irregular bursting and a dose-dependent increase in amplitude (Cazalets et al., 1992; Cowley & Schmidt, 1994; Jiang et al., 1999). In mice, 5-HT exerts an excitatory effect on CINs throughout neonatal development (Abbinanti et al., 2012). Given that V3 INs are a major population of glutamatergic commissural neurons (Borowska et al., 2013; Zhang et al., 2008), 5-HT may similarly enhance their intersegmental coupling by increasing excitatory drive across the midline.

### 1.6.2 N-methyl-D-aspartate (NMDA)

NMDA receptor activation alone can evoke rhythmic bursting in spinal networks by promoting voltage-dependent depolarization through $Ca^{2+}$ and $Na^{+}$ influx (Cazalets et al., 1990; Grillner et al., 1981). The $Mg^{2+}$-dependent block of NMDA receptors introduces a regenerative component to the cycle, generating rhythmic oscillations even in the absence of synaptic input (Nowak et al., 1984; Wallen & Grillner, 1987). These oscillations arise as membrane depolarization relieves the $Mg^{2+}$ block, allowing $Ca^{2+}$ influx that subsequently activates $Ca^{2+}$-dependent $K^{+}$ currents, leading to repolarization and the next depolarizing phase. Relief of $Mg^{2+}$ block is responsible for the region of negative slope conductance. In the absence of $Mg^{2+}$ the channel adopts an ohmic behavior. The interplay between these inward and outward currents

produces intrinsic rhythmic membrane oscillations that can lead network locomotor activity (Hernandez et al., 1991).

Beyond its intrinsic oscillatory effects, by increasing intracellular $Ca^{2+}$, NMDA strengthens propagation of excitatory drive amongst local and intersegmental circuits, strengthening coupling between rhythm-generating modules (Beato & Nistri, 1999). The frequency of NMDA-induced locomotor output is concentration-dependent, with higher NMDA levels increasing burst frequency, but compromising intersegmental coordination (Cazalets et al., 1992). In a small subset of V3 INs, NMDA-induced depolarization can elicit oscillations in membrane potential even when synaptically isolated (Zhang et al., 2008); however, the concentrations required to induce this state are substantially higher than those likely present under physiological conditions. These findings suggest that NMDA receptor activation in V3 interneurons primarily produces a sustained depolarization that lowers action potential threshold and increases excitability, rather than acting as a physiologically relevant intrinsic rhythmogenic mechanism. Although high concentrations of bath-applied NMDA can evoke membrane oscillations in a subset of synaptically isolated V3 interneurons (Zhang et al., 2008), these conditions differ substantially from the phasic, synaptically driven activation expected during locomotion. Consequently, the precise role of NMDA receptor activation in V3 interneuron recruitment during ongoing locomotor activity remains incompletely defined.

### 1.6.3 Dopamine (DA)

DA alone produces slow and irregular rhythmic activity but, when combined with 5-HT, stabilizes locomotor output (Kiehn & Kjaerulff, 1996; Lapointe et al., 2009). Therefore DA, in the context of locomotor-like rhythmic activity, is primarily used to stabilize ongoing locomotion, rather than initiate it. Acting via D1-like receptors, DA enhances persistent inward currents and

modulates membrane excitability, while D2-like receptors can dampen inhibitory inputs through opposing cyclic AMP actions (Bertran-Gonzalez et al., 2008). Specifically, low concentrations of DA, when added to preexisting rhythmic activity evoked via 5-HT and NMA, stabilizes and slows the rhythm frequency (Sharples et al., 2015).

At the network level, dopaminergic modulation enhances locomotor network performance by refining synaptic efficacy and balancing excitation and inhibition. DA also contributes to the maturation and flexibility of locomotor patterns during development, influencing how the spinal CPG transitions between different motor states (Sharples et al., 2015). DAs effect on V3 INs is not fully characterized, although it likely fine-tunes their excitatory drive and contributes to the robustness of the locomotor rhythm.

### 1.6.4 Combined Neurotransmitter Application in Fictive Locomotion

In isolated neonatal mouse spinal cord preparations, stable fictive locomotor activity is typically induced by combined application of 5-HT, NMDA, and DA, reflecting the synergistic neuromodulatory actions of these transmitters on spinal IN networks (Cazalets et al., 1992; Sharples et al., 2015; Whelanet al., 2000). The precise concentrations required vary slightly between studies and species; however, effective ranges generally include 5-HT at 5–35 μM, NMDA at 4–8 μM, and DA at 10–50 μM (Dougherty & Kiehn, 2010; Gosgnach et al., 2006; Hinckley et al., 2005; Zhang et al., 2008).

When applied together, these agents elicit a consistent, alternating left–right and flexor–extensor bursting pattern in ventral root recordings. NMDA provides the depolarizing drive necessary for rhythmogenesis, 5-HT enhances neuronal excitability and intersegmental coupling, and DA stabilizes and refines the rhythm by modulating intrinsic conductances and synaptic gain.

The combined application thus recapitulates descending monoaminergic and glutamatergic inputs that normally activate the locomotor CPG in vivo (Jordan et al., 2008).

The rhythmic pattern is sensitive to both the absolute and relative concentrations of these transmitters: excess NMDA can accelerate burst frequency and disrupt coordination, while elevated 5-HT or DA may slow or suppress rhythmicity (Jiang et al., 1999; Whelan et al., 2000). Therefore, achieving stable fictive locomotion requires balancing excitatory drive with modulatory tone to mimic the physiological activation state of the spinal locomotor network.

### 1.7 Project Rationale

Computational modeling studies have postulated that spinal V3 INs play a pivotal role in facilitating speed-dependant interlimb synchronization, thereby stabilizing locomotion across varying gaits and speeds (Zhang et al., 2022). Consistent with these predictions, locomotion in genetically modified adult mice lacking V3 INs is characterized by inappropriate left-right phasing and impaired coordination, particularly at higher locomotor speeds (Zhang et al., 2022). In parallel, experimental work has demonstrated that V3 INs are rhythmically active during fictive locomotion and contribute to motor neuron recruitment in zebrafish larvae, supporting a conserved role for this population in locomotor network function (Wiggin et al., 2022). Importantly, emerging evidence suggests that the V3 IN population is functionally heterogeneous, with evidence in mouse models showing a significant increase in the activity of c-fos positive dorsal V3 INs, tripling post-running, while c-fos positive ventral V3 IN activity doubled following both running and swimming (Borowska et al., 2013). These findings raise the possibility that ventral V3 INs may be more broadly engaged across locomotor contexts, potentially contributing to core CPG functions. Given the ventral localization of extensor-related premotor circuitry (McCrea & Rybak, 2008) and the excitatory, commissural projection patterns of V3 INs (Zhang et al., 2008), ventral V3 IN

populations are well positioned to reinforce ongoing motor output rather than initiate phase transitions. This organization suggests that ventromedial V3 INs would preferentially exhibit in-phase activity with ipsilateral extensor-related VR output during fictive locomotor-like states.

The physiological and electrophysiological properties of V3 INs indicate they have largely linear frequency-current response curves and moderate spike frequency adaptation, with a small subset displays intrinsic properties consistent with pacemaker-like activity (Borowska et al., 2015; Zhang et al., 2008). However, despite these proposed regulatory and integrative roles within the locomotor CPG, direct empirical characterization of the intrinsic electrophysiological properties and firing behaviour of V3 INs during locomotor CPG network activation remains limited.

Although the spinal locomotor CPG is often discussed in the context of rhythmic pattern generation, network activity during locomotion also includes substantial tonic excitatory drive that sets the gain and recruitment of spinal interneurons and motoneurons (Kiehn, 2016; McCrea & Rybak, 2008). Commissural excitatory interneurons, such as V3 interneurons, are well positioned to contribute to this tonic drive due to their projection patterns and sustained firing properties, while still being subject to rhythmic modulation during locomotor-like activity (Borowska et al., 2015; Zhang et al., 2008; H. Zhang et al., 2022). Accordingly, V3 interneurons may support locomotor output through a combination of tonic activity that stabilizes network excitability and phasic modulation that aligns their output with the locomotor cycle (Dougherty & Kiehn, 2010).

Therefore, the primary objective of my thesis is to characterize the intrinsic firing properties and excitability of V3 INs using whole-cell patch-clamp (WCPC) recordings in neonatal Sim1CreTdTom mice (P1-P5) during locomotor-like network activation characterized by rhythmic VR output as well as tonic network activation characterized by and increased and sustained VR output. By defining how V3 INs intrinsic properties are modulated under locomotor-

like conditions, this work aims to provide a cellular-level framework for understanding how distinct V3 sub populations may be recruited and contribute to spinal locomotor networks.

## 1.8 Aims and Hypotheses of Study

### 1.8.1 Overarching Hypothesis

Due to their electrophysiological properties, location, and projection patterns, we hypothesize that V3 INs will be rhythmically active during locomotion, likely because they help to establish robust and appropriately coordinated motor patterns.

### 1.8.2 Aim of Study

The aim of this thesis was to characterize the activity profile of V3 IN subpopulations at baseline and during rhythmic locomotor-like VR activity using WCPC recording. We additionally aimed to determine whether a particular V3 subpopulation is active in phase with either extension or flexion, in the step cycle.

### 1.8.3 Specific Aims and Hypotheses

**1)** Characterize the activity pattern of V3 INs during tonic motor activity.

   a. **Hypothesis 1:** All subpopulations of V3 INs will display tonic activity during tonic motor activity.

**2)** Characterize the activity pattern of V3 INs during drug-induced rhythmic locomotor-like activity.

   a. **Hypothesis 2:** All sub populations of V3 INs will display rhythmic activity during drug-induced fictive locomotor-like VR activity.

   b. **Hypothesis 3:** The ventromedial population will be in-phase with ipsilateral extension.

**3)** Determine if rostro-caudal location of V3s contributes to V3 altered activity during drug-induced fictive locomotor-like activity.

   **a. Hypothesis 4:** V3s located in the thoracic region of the spinal cord will display biphasic rhythmic activity during each step cycle.

   **b. Hypothesis 5:** V3s located in the lumbar region of the spinal cord will display rhythmic discharge correlated with activity in ipsilateral extensors in each respective ventral root.

# Chapter II: Material and Methods

## 2.1 Ethics Declaration

Animal experimental protocols conducted at the University of Manitoba and followed the Canadian Council on Animal Care guidelines and were approved by the university's Animal Ethics Committee.

## 2.2 Animal Models

*In vitro* optogenetic electrophysiological experiments were performed on a total of $n$ = 133 neonatal (P0-P7) mice of both sexes. The $Sim1^{Cre/+;}Rosa26^{floxtopTdTom/+}$ (Sim1TdTom; Zhang et al., 2008) and the $Sim1^{Cre/+}$; $Rosa26^{floxstopTdTom/+/Gt(Rosa)26floxstopH134R/EYFP/+}$ (Sim1TdTom/ChR2; Chacon et al., 2023) lines were used to visualize V3 INs under fluorescent microscopy. All experiments were conducted with mice bred within the University of Manitoba's Genetic Models Center, and preparation numbers and types (slice, thoracic cut or dorsal horn removed) are described below.

## 2.3 Solutions Preparation

### 2.3.1 Dissecting Solution

Dissecting solution contained: KCl, 3mM; $NaHCO_3$, 25mM; $KH_2PO_4$, 1.2mM; $MgS0_4$, 1.3mM; $CaCl_2$, 1.2mM; glucose, 10mM; sucrose, 212.5mM; $MgCl_2$, 2mM; with a pH of 7.4. Was oxygenated with 95% $O_2$ and 5% $CO_2$ gas for 15 minutes prior to use and was maintained at a temperature <4 °C, as colder temperatures are thought to enhance a tissues survival rate through reduced metabolism and oxygen demand.

### 2.3.2 aCSF Ringer Solution

Artificial cerebrospinal fluid (aCSF) Ringer's solution contained: NaCl, 111mM; KCl, 3.1mM; glucose, 11mM; $NaHCO_3$, 25mM; MgSO4, 1.25mM; $CaCl_2$, 2.5mM; $KH_2PO_4$, 1.8mM; with a pH of 7.4. Solution was prepared 30 minutes prior to dissection to allow for complete oxygenation and homogenization of the solution.

### 2.3.3 Pipette Intracellular Solution

**a. P5+ Intracellular Solution:**

K-Methane Sulphonate, 0.14mM; NaCl, 0.01mM; $CaCl_2$, 0.001mM; HEPES, 0.01mM; ATP, 0.003mM; GTP-Li, 0.0004mM; EGTA, 0.01mM; with a pH of 7.2.

**b. P0 – P4 Intracellular Solution:**

K-gluconate, 128mM; HEPES, 10mM; $CaCl_2$, 0.0001mM; glucose, 1mM; NaCl, 4mM; Mg-ATP, 5mM; GTP, 0.3mM; with a pH of 7.4.

## 2.4 Slice Preparation

Slice preparations were obtained from the caudal thoracic to caudal lumbar spinal cord (T11–L6) of P0–P7 mice ($n$ = 14). Animals older than P5 were briefly anesthetized with isoflurane (Fresenius Kabi Canada Ltd, ON, Canada) until loss of the righting reflex. P4 and younger mice were not anesthetized. Animals were decapitated at the medulla-spinal cord junction and pinned ventral side up in a Sylgard-coated dissecting dish. Spinal cords were dissected out in an ice-cold (<4 °C) oxygenated (95% $O_2$/5% $CO_2$) dissecting solution (in mM: KCL, 3; $NaHCO_3$, 25; $KH_2PO_4$, 1.2; $MgS0_4$, 1.3; $CaCl_2$, 1.2; glucose, 10; sucrose, 212.5; $MgCl_2$, 2; pH7.4), encased in low-melting point agarose (Sigma-Aldrich Cat# A4018) and sectioned transversely at 300microns on a vibratome (Leica VT1200S, Leica). Slices were then transferred to incubated (30°C) recovery chambers (Model 7470, Campden Instruments), oxygenated Ringer's solution (in mM: NaCl, 111;

KCl, 3.1; glucose, 11; $NaHCO_3$, 25; $MgSO_4$, 1.25; $CaCl_2$, 2.5; $KH_2PO_4$, 1.8; pH 7.4), according to their spinal section, and allowed to recover for 30 minutes prior to electrophysiological experiments.

**2.5 Slice Mounting for Electrophysiological Recording**

Post incubation, slices were transferred and secured to a clean 15mL clear recording chamber superfused with oxygenated ringer aCSF (raCSF). Slices were anchored to the chamber with a flat framed platinum harp (SHD – 42/15). Chamber was then secured under a Zeiss Axio Imager Z.2 upright microscope.

**2.6 Whole Spinal Cord Preparation**

Neonatal mice ($n$ = 119) of both sexes were decapitated at the medulla-spinal cord junction and pinned ventral side up in a sylgard-coated dissecting dish. With the dorsal aspect fully submerged in cold (<4 °C) oxygenated (95% $O_2$/5% $CO_2$) dissecting solution. The pup was eviscerated to expose the ventral aspect of the vertebral column. A whole-cord, ventral laminectomy was performed. Dorsal roots were cut while ventral roots were sparred during isolation of the spinal cord. Once the spinal cord was isolated, the outer meninges were removed to optimizes oxygenation and drug absorption through the entire cord, as well as make it more accessible for additional transections. Following removal of the meninges, the cord was cut for either the thoracic exposed or dorsal horn-removed preparation as described below.

### 2.6.1 Thoracic Exposed Preparation

The whole cord ($n$ = 81), rostral cervical to caudal sacral, was secured with acrylic glue and petroleum jelly to a specimen disc, ventral side up on a 45° agar 'pillow', in room temperature (23-25°C) oxygenated (95% $O_2$/5% $CO_2$) aCSF solution. The disc was then mounted inside the vibratome chamber, such that the sectioning proceeded in a caudal-to-rostral direction and filled with ice cold (<4 °C) aCSF. The cut was completed using a vibratome (Leica VT1200S, Leica) at the level of T6-T3 (**Figure 4**). Because the spinal cord was already angled on the agar support, subsequent horizontal vibratome sectioning produced a 45° cut over 3 spinal segments, a configuration that preserves motor neuron axons and increases the visualized surface area. It was then transferred to a sylgard-lined 15mL recording chamber and superfused with oxygenated (95% $O_2$/5% $CO_2$) aCSF.

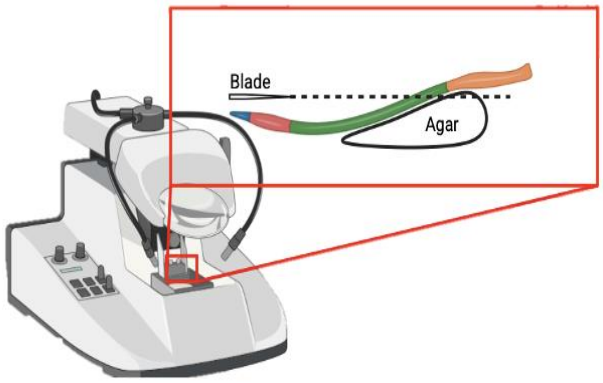


**Figure 4.** Thoracic exposed spinal cord preparation showing orientation of spinal cord in relation to vibratome blade to ensure large oblique cut over multiple rostral thoracic segments (T6 – T3) (Created with BioRender.com, 2025).

### 2.6.2 Dorsal Horn Removed Preparation (Dougherty et al., 2013b)

The whole cord ($n$ = 38) was secure on its side to a specimen disc and pinned at its most rostral and caudal ends. Using a 15° stab knife, a cut was made along the longitudinal lateral-medial line (**Figure 5, A**), demarcating the ventral from the dorsal aspect (**Figure 5, B**). The cord

was then transferred to a sylgard-lined 15mL recording chamber with oxygenated (95% $O_2$/5% $CO_2$) aCSF and pined ventral side down, exposing cut mid-section.

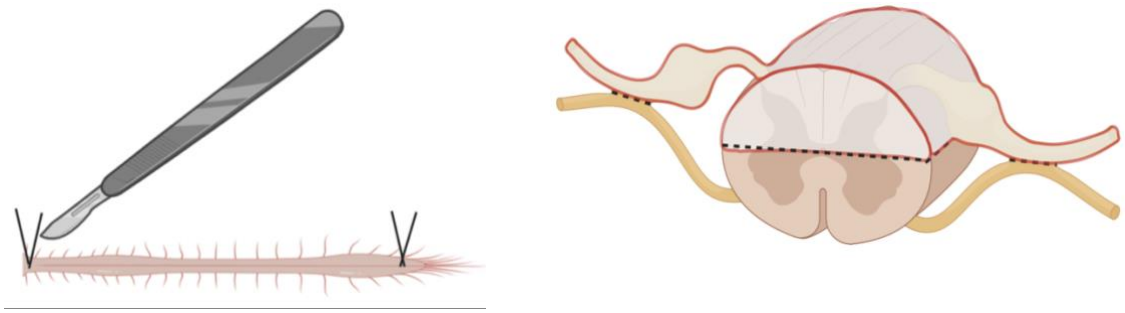

**A)** **B)**

**Figure 5.** Dorsal horn–removed spinal cord preparation illustrating the pinning and orientation of the cord during dissection. **A)** The spinal cord was pinned and stabilized along its lateral side before sectioning along the longitudinal lateral-medial line with a scalpel. **B)** The entire dorsal aspect of the spinal cord, including dorsal roots, was removed to expose the ventral surface for subsequent recordings (Created with BioRender.com, 2025).

### 2.7 Whole Cord Mounting for Electrophysiology

The preparations were then transferred and secured to a clean 15 mL clear recording chamber, which was then placed under the Zeiss Axio Imager Z.2 microscope, ventral side up, and continuously superfused with oxygenated raCSF (**Figure 6**). To further stabilize the spinal cord for recording, the caudal end was gently pinned to the chamber. Suction electrodes were used to record from L5 and L2. A gravity-dependant perfusion system (ValveLink 8.3, Automate Scientific Inc, CA, USA) superfused the preparation continuously with oxygenated (95% $O_2$/5% $CO_2$) raCSF. A peristaltic pump (Minipuls 3 Peristaltic Pumps, Gilson, WI, USA) collected and recycled excess aCSF.

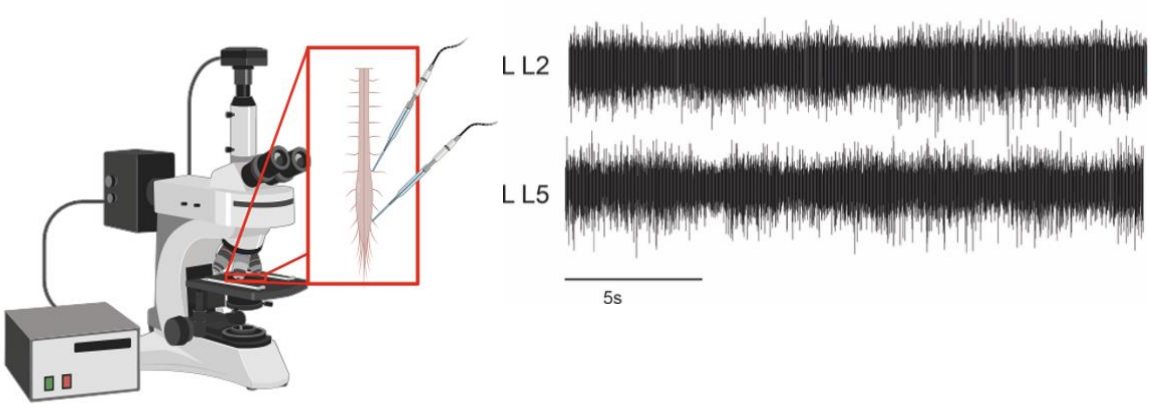


**Figure 6.** Illustration showing the mounted spinal cord preparation used for VR recordings (left). Representative traces showing alternating rhythmic locomotor-like activity recorded from the left lumbar (L) VR L2 (top trace) and L5 (bottom trace) during rhythmic locomotor-like activity (Created with BioRender.com, 2025).

### 2.8 Induction of Rhythmic Locomotor-Like Activity in Spinal Cord Preparations

Glass suction electrodes were prepared for recording electrical activity from the lumbar ventral roots. Thin-walled borosilicate glass capillaries with microfilament (outer diameter 1.2 mm, inner diameter 0.90 mm; A-M Systems Inc., WA, USA) were pulled on a vertical puller (Narishige Scientific Instrument Laboratory, Tokyo, Japan). The resulting fine tips were blunted against a sharpening stone (Dan's Whetstone Company Inc., AR, USA) and subsequently smoothed using a flame from a compact alcohol burner (Boekel Industries Inc., PA, USA). The final tip diameter was adjusted to approximately 110 – 120 µM through repeated gentle filing and fire-polishing.

The suction electrodes were applied to the L2 and L5 ventral roots (VR), as these roots are known to correlate to the flexion and extension phases of the step cycle (Zaporozhets et al., 2004), however, alternative roots such as L3 and L6 were also used if required as, although less robust, these roots still have potential to demonstrate rhythmic activity. Negative pressure was generated manually with the syringe to draw the root into the electrode tip and establish a stable seal. VR signals were then assessed for baseline noise fluctuations and recording artifacts. Signals (20–50 µV at 1000x gain) were then amplified 10,000x, band-pass filtered between 30–3000 Hz using a

custom SCRC amplifier and digitized at 2000 Hz with a CED Power 1401 A/D interface and Signal software (Cambridge Electronic Devices, Cambridge, UK).

Neurochemicals for inducing rhythmic locomotor-like activity in the VRs were made in bulk prior to experiments and stored in freezer. Varying combinations and concentrations of 5-hydroxytryptamine (5-HT, Sigma-Aldrich Co., MO, USA; 20 – 35 μM), N-methyl-D-aspartic acid (NMDA, Sigma-Aldrich; 5 μM), and dopamine (DA, Sigma-Aldrich; 5 μM) were used depending on age of the pup. Total concentration of individual neurochemicals used per experiment refers to final total bath concentration. Neurochemicals were mixed into a 25 mL of raCSF. After the perfusion line was cleared, the solution was oxygenated and introduced into the gravity-fed perfusion system to evoke locomotor-like rhythmic activity in the spinal cord. Circulation was maintained by a suction line that returned excess solution to the reservoir for continuous recirculation. The roots were either re-suctioned to improve the seal, or the drugs were washed out. Washout was performed by clearing all neurochemicals from the perfusion system and replacing the drug-containing solution with fresh oxygenated raCSF until VR activity returned to baseline. Once washout was achieved, the drug-containing solution (as described above) was reintroduced into the perfusion system.

Tonic VR activity was defined as a sustained elevation in discharge above baseline, whereas the desired locomotor-like rhythmic activity was identified as bursts of VR discharges. Rhythmic activity was characterized by alternating fluctuations between ipsilateral L2 and L5 VRs, or by bursting that occurred in-phase across contralateral L2 and L5 VRs. These patterns reflect the functional roles of L2 and L5, which correspond to the flexion and extension phases of the step cycle, respectively (Cowley & Schmidt, 1994; Kjaerulff & Kiehn, 1996).

## 2.9 Whole Cell Patch Clamp Recordings and Stimulations

Borosilicate glass capillary tubes were pulled using a horizontal micropipette puller (Sutter Instrument P-97, Micropipette Puller for Microinjections) to achieve a resistance of 7-10MΩ. The pipette was then filled with intercellular solution according to age of the pup (as mentioned above). Targeted V3 neurons were identified under fluorescence, and once a cell was selected, the pipette was advanced under visual guidance for precise approach. A giga-seal was confirmed by a sudden increase in pipette resistance from MΩ to GΩ (**Figure 7, A)**. Following seal formation, gentle negative pressure was applied through a syringe-driven system to rupture the membrane and establish whole-cell access (**Figure 7, B**). Cellular properties were assessed using a series of depolarizing and hyperpolarizing current pulses (described below) while holding the membrane potential at –60 mV to ensure a consistent baseline across recordings. When neurons were patched prior to drug application, recordings were obtained once under baseline conditions and again during drug exposure. If the cell remained stable, a washout was then performed to return activity to baseline.

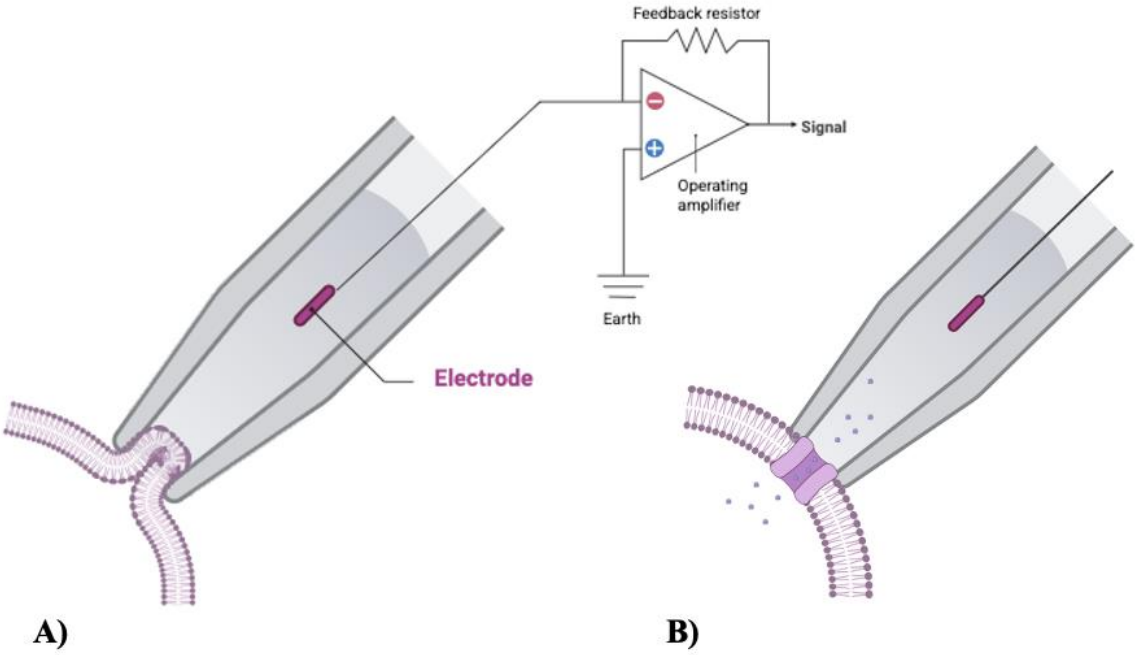


**Figure 7.** Whole-cell patch-clamp recording configuration. A) Recording electrode forms a *gigaseal* by tightly adhering to the cell membrane prior to membrane rupture. B) Following membrane breakthrough, the electrode gains access to the cell's interior, establishing the whole-cell configuration for recording transmembrane currents and potentials (Created with BioRender.com, 2025).

### 2.10 Electrophysiological Protocols for Assessing Intrinsic and Firing Properties of V3 INs

Electrophysiological protocols to observe the response patterns and electrophysiological properties of V3 INs at baseline and post application of neurochemicals included rheobase, depolarizing steps current step injections, and hyperpolarizing current step injections. Recordings were performed under both current- and voltage-clamp configurations to characterize intrinsic membrane properties and spontaneous neuronal activity. Alternation in excitability of V3 was reflected by changes in resting membrane potential (RMP), Rheobase, input resistance ($R_{in}$), and firing frequency (FF), while secondary markers of neural excitability included hyperpolarization sag amplitude (HSA), and post-inhibitory rebound potentials. All protocols were performed while holding the cell at −60 mV to ensure consistency across recordings.

### 2.10.1 Rheobase

The rheobase of a neuron is characterized as the minimum amount of current needed to evoke an action potential 50% of the time, in response to increasing 10ms depolarizing current steps (Chopek et al., 2018) (**Figure 8).** Neuronal excitability was considered increased when rheobase values decreased following drug application, indicating that less current was required to elicit an action potential.

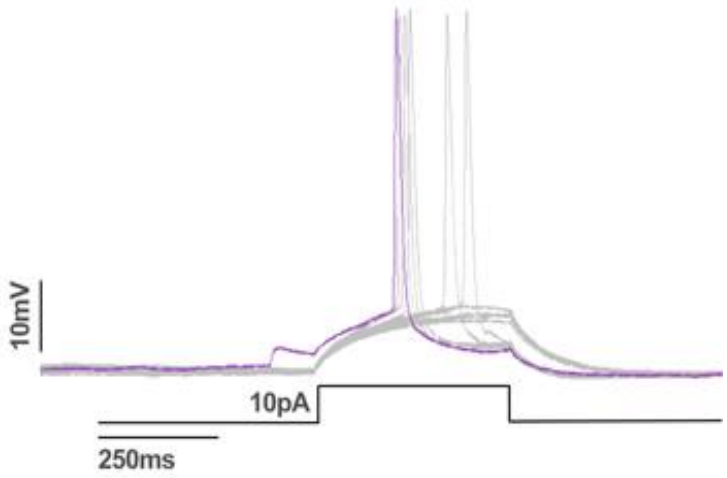


**Figure 8.** Representative trace showing the rheobase of a neuron responding to a 10pA depolarizing current step (500ms duration). The single action potential elicited at this threshold reflects the minimal current required to evoke neuronal firing.

### 2.10.2 Firing Frequency

The steady-state FF of each neuron was determined using 1-s depolarizing current step injections, with current amplitude incremented by 10 pA between runs (**Figure 9**). Following analysis of all 27 datasets, frame 12 was selected as a consistent reference point, as it most reliably represented stable neuronal firing patterns across recordings. For each depolarizing current step, the total number of action potentials (spikes) were counted and then divided by the duration of the current pulse to calculate the firing frequency.

The firing frequency ($f$) was calculated as:

$$f = \frac{N}{\Delta t}$$

where **N** is the number of action potentials and **Δt** is the duration of the depolarizing current step (in seconds). An increase in neuronal excitability was defined as an elevation in $f$, reflecting a greater number of action potentials generated in response to the same depolarizing current input

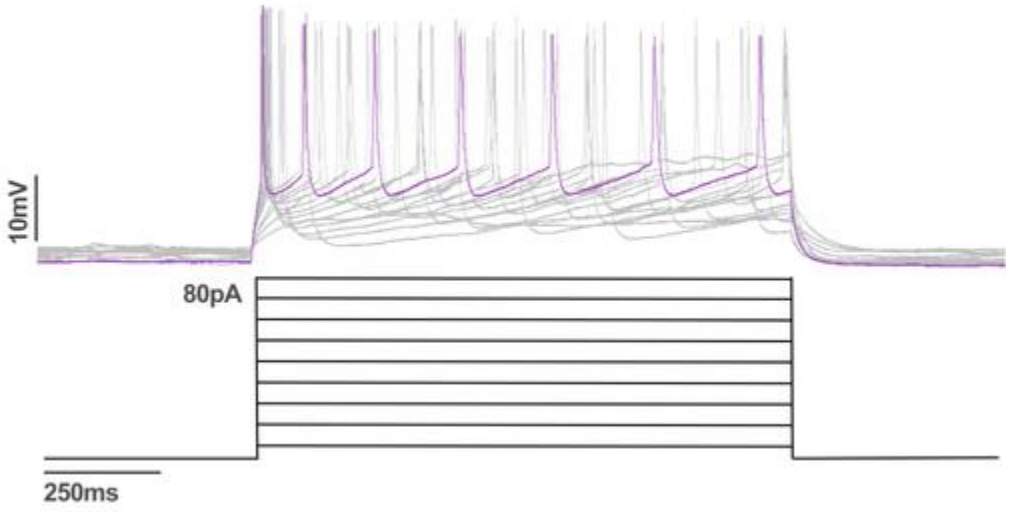


**Figure 9.** Representative trace of a neuron firing in response to a 10 pA depolarizing current step, which increases by 10pA every run. Note the figure shows an example of 8 current steps. The trace shows a sustained train (tonic) of action potentials evoked during a 1-s current injection, demonstrating the steady-state FF ($f$) of the neuron under this stimulation intensity.

### 2.10.3 Hyperpolarization Sag Amplitude (HSA)

The sag response is a gradual, time-dependent depolarization that occurs in response to a hyperpolarizing current injection, in which the membrane potential shifts toward its baseline RMP from its initial hyperpolarized state (**Figure 10**). This depolarizing 'sag' is mediated by the

$I_h$ cationic current, which is thought to be activated during membrane hyperpolarization to restore the neuron towards its baseline potential (Dougherty & Kiehn, 2010). To quantify sag amplitude, neurons were subjected to a hyperpolarizing step protocol consisting of 1s negative current injections, with current amplitude increased by 10 pA between successive runs for a total of 20 runs. Following analysis of all 27 datasets, frame 10 was selected as a consistent reference point, as by this time the neuron exhibited a stable and fully developed sag response with minimal baseline fluctuation. Sag amplitude was quantified as the voltage difference between the peak membrane hyperpolarization in response to a negative current step and the steady-state potential reached before the end of the pulse. A neuron was considered to have increased excitability if the sag amplitude increased post neurochemical application, indicating enhanced activation of hyperpolarization-activated cyclic nucleotide-gated (HCN) channels such as $I_h$ currents.

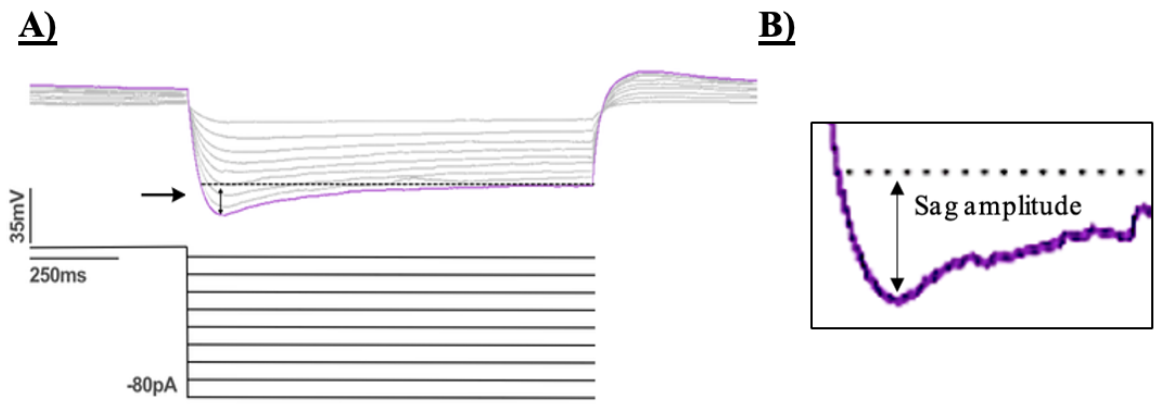


**Figure 10.** A) Representative trace of the sag response of a neuron during a hyperpolarizing current injection. A 1s, −10 pA current step produced an initial hyperpolarization followed by a gradual depolarizing "sag" (arrow) toward the RMP. Following current injections increase by 10pA every run. B) Expanded view of the area of measurement.

### 2.10.4 Postinhibitory Rebound

The postinhibitory rebound (PIR) potential is the peak depolarization that occurs immediately after the termination of a hyperpolarizing current (**Figure 11**). The PIR is related to deactivation of $I_h$ and/or a transient calcium current, $I_T$, which then causes the neuron to exhibit a rebound depolarization that can sometimes reach threshold to trigger an action potential. PIR amplitude was quantified as the peak depolarization following release form a hyperpolarizing current step, and measured as the peak voltage of the action potential produced. Subthreshold rebound depolarizations that did not elicit action potentials were not included in PIR amplitude analysis. V3 INs were subjected to 20 hyperpolarizing steps protocols consisting of 1s negative current injections, with current amplitude increased by 10 pA between successive runs. Following analysis of all 27 datasets, frame **9** was selected as a consistent reference point, as by this time the neuron exhibited a stable and fully developed PIR response with minimal baseline fluctuation. A neuron was considered to have increased excitability if the PIR amplitude increased relative to baseline, suggesting increased rebound depolarization capacity.

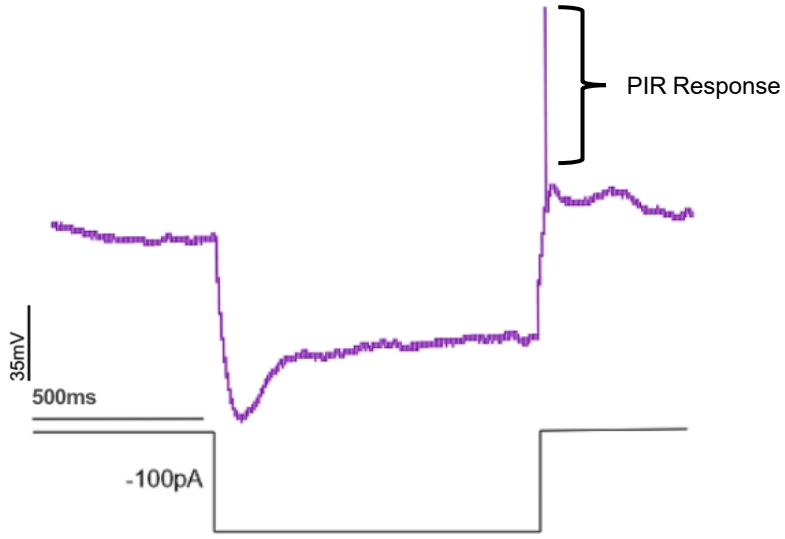


**Figure 11.**Representative trace of a PIR response of a neuron during a hyperpolarizing current injection. Once the 1s, −100 pA current step is released, the neuron produces a PIR potential that is enough to evoke a rebound action potential.

### 2.10.5 Input Resistance

Input resistance ($R_{in}$) was determined by injecting a series of small, 500ms negative current injections of -10pA, and measuring the corresponding steady-state membrane potential deflections (ΔV) (**Figure 12**). $R_{in}$ (MΩ) was calculated as the slope of the linear portion of the ΔV–ΔI relationship, according to the equation:

$$R_{in} = \frac{\Delta V}{\Delta I}$$

where ΔV represents the change in membrane potential (mV) and ΔI represents the injected current (pA). A neuron was considered to have increased excitability if its $R_{in}$ increased, as this reflects a reduction in total membrane conductance, and increased likelihood of reaching its voltage threshold for an action potential.

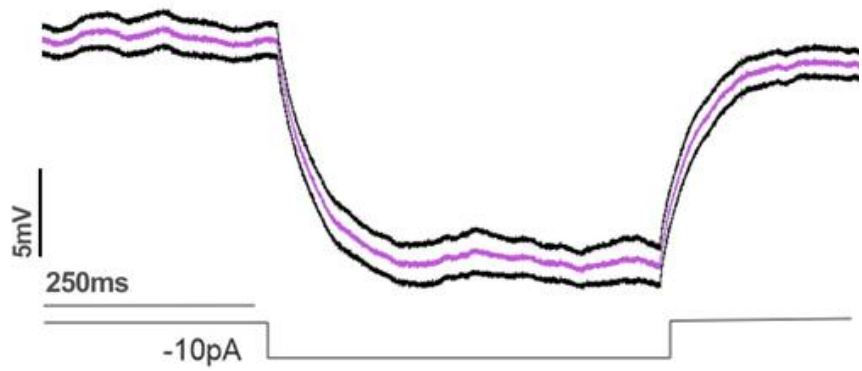


**Figure 12.**Representative trace used to calculate neuronal $R_{in}$. A series of hyperpolarizing current steps (−10 pA) were applied in current-clamp mode to measure steady-state voltage deflections. The traces above and below (black) represent the error bar, while the averaged response (purple) illustrates the consistent voltage deflection used for $R_{in}$ determination.

### 2.11 Data Analysis

Data are presented as means ± SD unless otherwise noted. These experiments were exploratory in nature; therefore, no statistical methods were used to predetermine sample size, and no randomization or blinding was performed. Analyses were limited to descriptive measures, basic calculations as described below, and graphical representations, which were carried out using GraphPad Prism (GraphPad Software, CA). No formal statistical comparisons were applied.

# Chapter III: Results

A total of 133 mice were used for experimentation, of which 21 preparations produced stable whole-cell recordings from 27 V3 INs with measurable firing activity and were included in subsequent analyses. Of these, rhythmic VR activity was evoked in one or more roots during WCPC recordings of a V3 IN in 8 thoracic exposed preparations. In 14 mixed preparations of thoracic exposed ($n$ = 3) and dorsal horn-removed ($n$ = 10), tonic VR activity was evoked during WCPC recordings of V3 INs. The remaining preparations were used to study the effects of pharmacological agents applied to induce rhythmic activity on V3 INs in slice preparations (n = 5) during WCPC recordings.

Among the 27 V3 INs, 17 included baseline and post-drug application recordings, 9 included post-drug recordings only, and only 1 included baseline recordings only. The remaining 106 preparations were excluded from analysis due to technical issues, including electrode malfunctions or excessive noise in VR recordings (n = 15), incomplete datasets or evidence of unhealthy neurons (n = 27), failure to evoke rhythmic VR activity (n = 35), or limitations in experimenter technique (n = 34). The number of trials per preparation varied depending on neuron viability at the exposed surface and the overall health of the spinal cord throughout the experiment. Despite the high exclusion rate, the remining preparations provided consistent and reproducible recordings.

### 3.1 Visualization of V3 INs

Using the $Sim1^{Cre/+;}Rosa26^{floxtopTdTom/+}$ transgenic mouse line, V3 INs expressing the transcription factor Sim1 were selectively labeled with the fluorescent reporter tdTomato**,** allowing for their clear identification within the ventral spinal cord. These fluorescently labeled neurons were visualized using a Zeiss Axio Imager Z.2 upright microscope equipped with a 20×

objective, providing sufficient resolution to distinguish individual soma and dendritic projections. The strong tdTomato signal enabled reliable targeting of V3 INs for WCPC recordings while preserving overall tissue integrity and spatial context within the preparation (**Figure 8**).

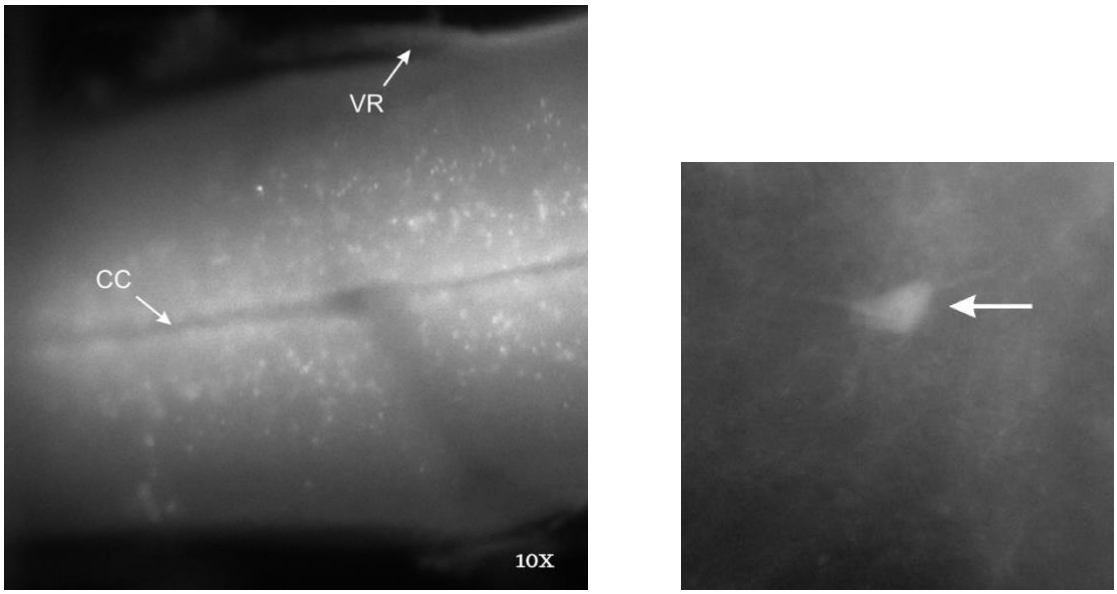


**A)** **B)**

**Figure 13.** Visualization of V3 INs using tdTomato reporter expression. **A)** 10× magnification of a dorsal horn–removed spinal cord preparation showing the exposed ventral surface, including the central canal (CC) and left VR at segment L1. **B)** 20× magnification with additional software zoom showing tdTomato-labeled V3 IN somas (arrows).

### 3.2 Neurochemical-Induced VR Activity

To examine the activity of V3 INs during rhythmic locomotor-like output, VR recordings were obtained to record activity resembling *in-vivo* motor patterns in the neonatal mouse spinal cord. Initial whole-cord experiments ($n = 45$) were conducted using the thoracic-exposed preparation in P1–P7 pups. Neurochemical application varied with age, ranging from [30 - 50 $\mu M$ 5-HT, 2.5 - 10 $\mu M$ NMDA] in pups ≤ P3, to [35 - 50 $\mu M$ 5-HT, 2.5 - 10 $\mu M$ NMDA, 5 - 30 $\mu M$ DA] in pups > P4. In many of these preparations ($n = 44$), VR activity began as tonic and remained tonic throughout the experiment, even when alternative roots were suctioned (Figure

14, B). This outcome was primarily attributed to two factors: (1) ongoing optimization of age-dependent neurochemical concentrations, and (2) limited technical proficiency of experimenters during early stages of the project. As viability of the preparations improved we found that using > 5 $\mu M$ of NMDA and/or the addition of DA, when the pup was P2 or younger, led to tonic root activity in all cases.

The concentrations that we found to be most successful in evoking some level of rhythmic VR output were [30 $\mu M$ 5-HT, 5 $\mu M$ NMDA] in pups ≤ P2, and [30 $\mu M$ 5-HT, 5 $\mu M$ NMDA, 5 $\mu M$ DA] in pups ≥ P3; successfully generating either disorganized or organized locomotor-like rhythmic VR bursting (**Figure 13. C - D**) 70% of the time (*n = 26*) in the remaining 37 preparations.

Although the dorsal horn–removed preparation (*n=38*) allowed improved visualization of the ventral surface and greater accessibility to V3 INs for WCPC recordings, it was ineffective at evoking rhythmic bursting as all preparations remained tonic under these experimental conditions. This limitation was likely due to increased tissue damage during dorsal horn removal, which may have disrupted the integrity and network dynamics of the CPG.

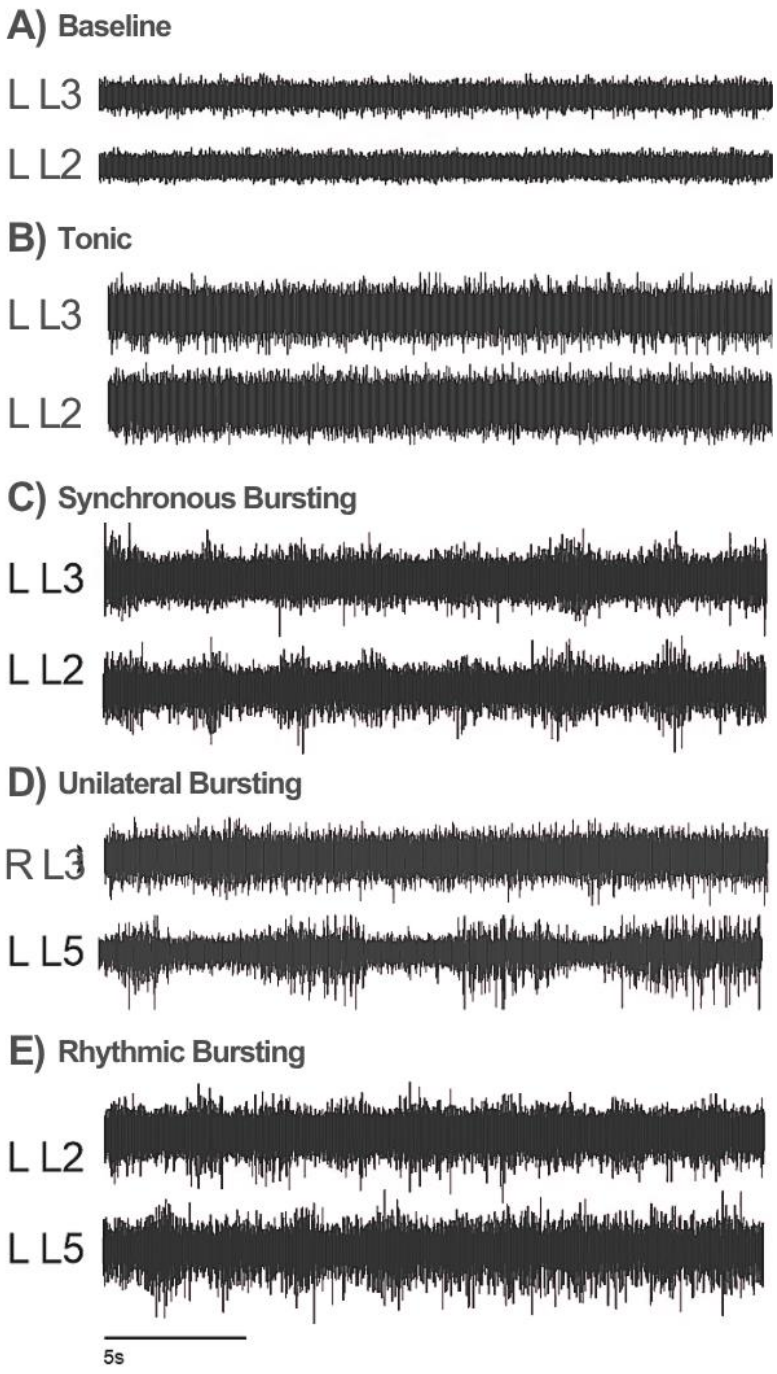


**Figure 14.** Representative extracellular recordings from lumbar ventral roots showing the range of network outputs observed following locomotor-inducing drug application. **A)** *Baseline*: low-amplitude spontaneous activity with no organized pattern. **B)** *Tonic*: sustained, non-rhythmic increases in activity amplitude. **C)** *Synchronous bursting*: two VRs exhibit simultaneous bursts without clear alternation. **D)** *Unilateral bursting*: rhythmic bursting restricted to one side while the contralateral segment remains tonically active. **E)** *Rhythmic bursting*: stable, alternating locomotor-like bursts between VRs.

### 3.3 V3 INs Exhibit Various Changes in Intrinsic Excitability Following Neurochemical Application

To assess how neurochemically induced locomotor conditions alter V3 IN properties, membrane and firing parameters were compared before and after bath application of 5-HT (30 $\mu M$), NMDA (5 $\mu M$), and DA (5 $\mu M$ for P $\geq$ 3 pups). Among all V3 INs neurons ($n = 17$), responses were variable. Approximately half of the cells (9/17) exhibited membrane depolarization from baseline ($\Delta$RMP = +11.6 ± 3.2 mV, mean ± SD), whereas the remainder hyperpolarized ($\Delta$RMP = -5.81 ± 6.4 mV, mean ± SD) (**Figure 15**). Consistent with a subset of neurons becoming excitable, 8/17 required less current to elicit an action potential (decreased rheobase) (Rheobase = -9.5 ± 4.2 mV, mean ± SD).

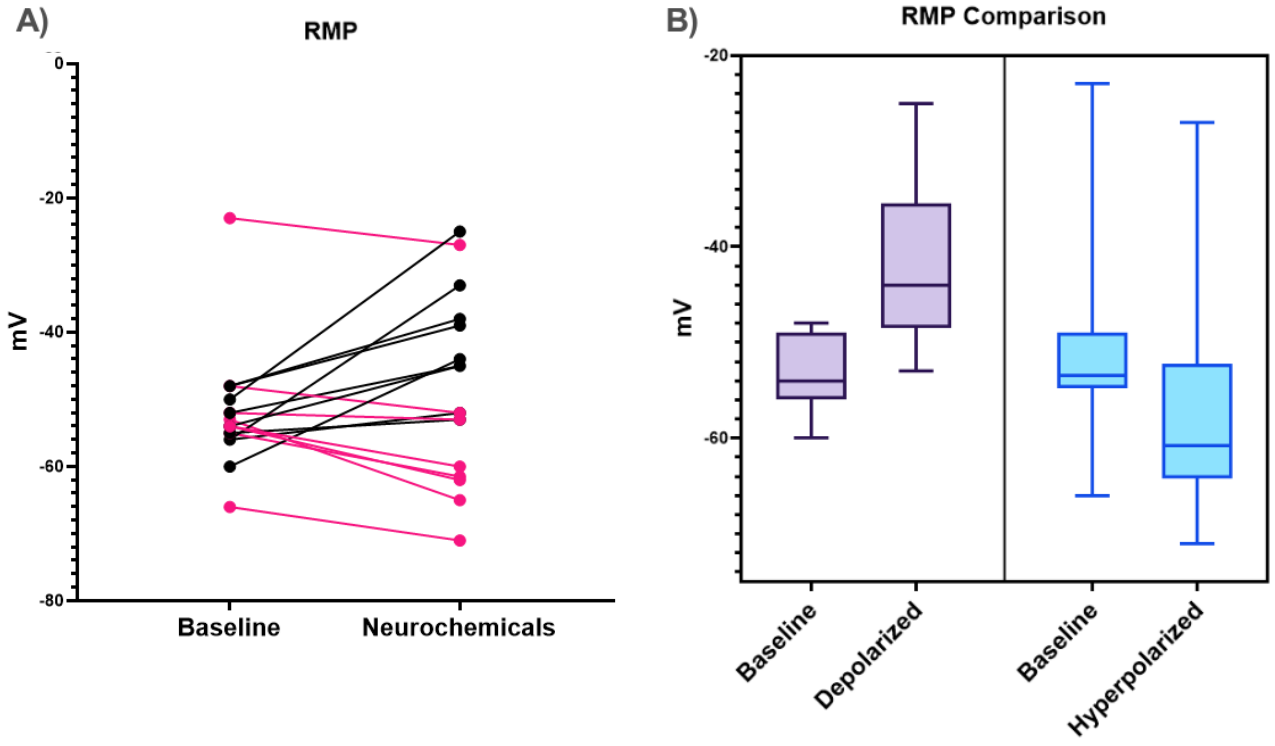


**Figure 15.** V3 INs exhibit different RMP responses following neurochemical application. A) Before-after plot showing the distribution of RMP values for all recorded V3 INs (n = 17) at baseline and after neurochemical application. Each point represents a single neuron, with bars connecting each neuron's responses. B) Box-and-whisker plots comparing neurons that

depolarized (purple, n = 9) versus those that hyperpolarized (blue, n = 8) in response to the neurochemical application, illustrating distinct subpopulations within the V3 cohort. Boxes represent the middle 50% of the diagram, with the midline representing the median of the data set and the vertical lines represent the max and minimum dataset points.

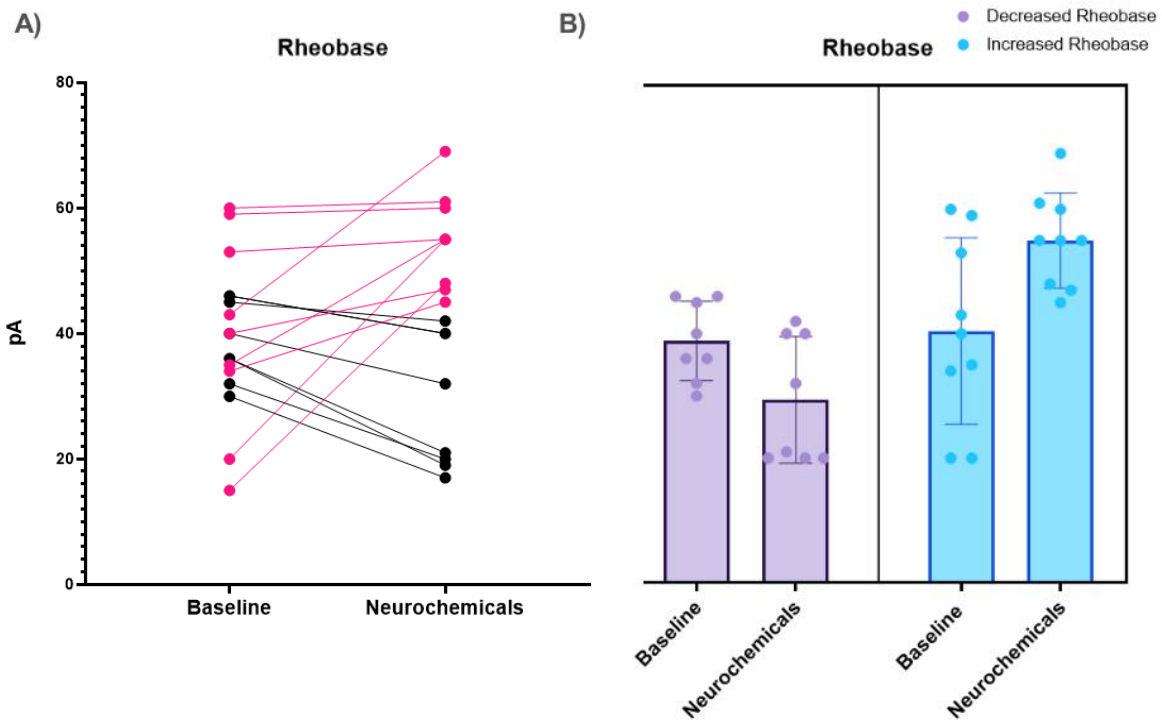


**Figure 16.** V3 INs exhibit differential changes in rheobase following neurochemical application. A) Scatter plot showing the distribution of rheobase values for all recorded V3 INs ($n$ = 17) at baseline and after neurochemical application. Each point represents a single neuron, with horizontal bars indicating mean ± SD. B) Bar plots show baseline and post-neurochemical rheobase values for neurons that decreased (purple, n = 8) or increased (blue, n = 9) in rheobase. Bars represent mean ± SD, with individual data points overlaid to illustrate variability. These opposing shifts highlight two distinct rheobase response profiles within the V3 population.

Among all recorded neurons ($n$ = 17), two distinct firing responses emerged following drug application: one group ($n$ = 8) exhibited increased firing frequency (ΔFF = 3.55 ± 2.7 Hz, mean ± SD), while the other ($n$ = 7) became completely shunted (**Figure 17, B**), only producing a single action potential, rather than a successive train of action potentials (**Figure 9**). A small subset of neurons ($n$ = 2) was considered non-adapting as there was no observed change of firing frequency when comparing baseline to post-drug conditions. These categorical shifts demonstrate that

locomotor inducing neurochemical can both recruit and suppress distinct V3 IN populations, reflecting differential modulation of intrinsic excitability within these subpopulations.

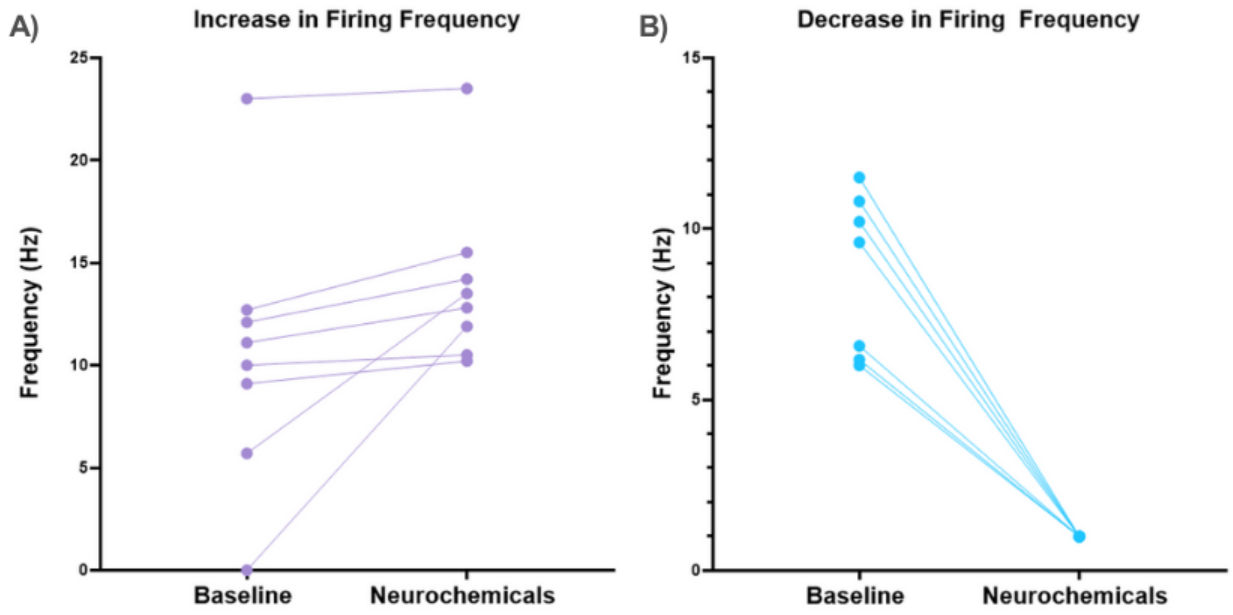


**Figure 17.** V3 INs exhibit differential changes in FF following neurochemical application. A) This graph shows the subset of neurons which increased their FF following bath application of locomotor inducing neurochemicals, indicating enhanced excitability. B) This graph shows the subset of neurons which completely lost the ability to fire successive trains of action potentials, transitioning from active at baseline to silent post-drug. Each line represents an individual neuron.

Among all recorded neurons (n = 17), neurochemical application produced a general decrease in $R_{in}$ (**Figure 18**). Most neurons (15/17) exhibited reductions in Rin, forming two clear subgroups: one showing moderate decreases of 8–20% (n = 8) and another showing large decreases of ≥ 49% (n = 7). The remaining two neurons instead displayed increases in Rin of 19% and 48%. This pattern reflects variable membrane responses to drug application within the V3 population.

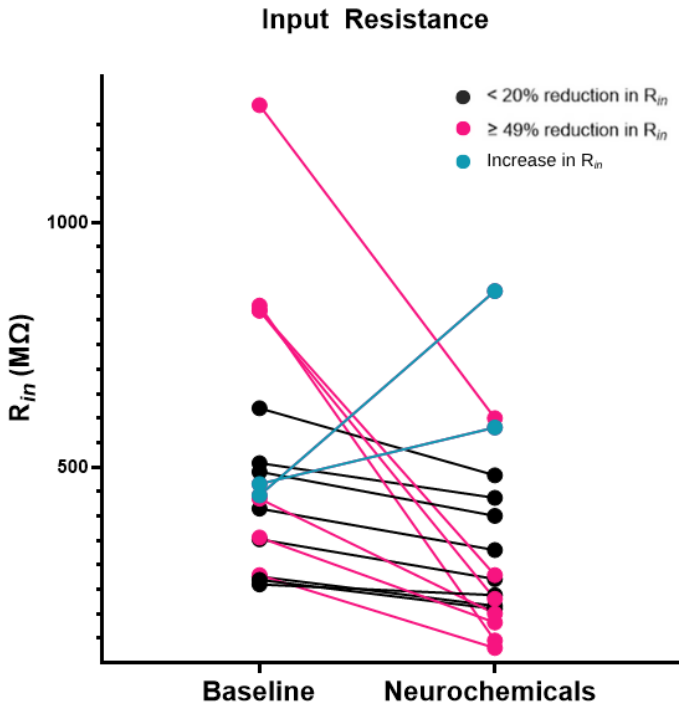


**Figure 18.** Neurochemical application decreased $R_{in}$ in most V3 INs. Paired data showing $R_{in}$ (MΩ) at baseline and following application of neurochemicals ($n$ = 17). Two subgroups were evident: neurons with a reduction of > 20% (black, $n$ = 8), and those with a reduction of ≥ 49% (pink, $n$ = 7). With one two neurons showing an increase in $R_{in}$ (blue).

Neuronal activity was measured in neurons prior to and following application of neurochemicals. Activity was classified as action potentials generated by a neuron with no experimental triggers in either current- or voltage-clamp mode, and silence was classified as no action potentials. Of the group of neurons that included baseline and post-neurochemical recordings ($n$ = 16), 5 neurons went from being silent at baseline to active post neurochemical application and 3 were active both at baseline and post-neurochemical application. In contrast, 3 neurons were active at baseline and were silent post neurochemical application, and 5 were silent in both conditions (**Table 1**). In a small subset of neurons recorded only post neurochemical

application ($n$ = 9) only 3/9 neurons were active. Out of the total group ($n$ = 25), 44% of the V3 INs became active following application of neurochemicals for rhythmic activity (**Table 2**).

| Baseline | Post-Neurochemicals | Total Neurons |
|---|---|---|
| Silent | Active | $n$ = 5 |
| Active | Active | $n$ = 3 |
| N/A | Active | $n$ = 3 |
| Active | Silent | $n$ = 3 |
| Silent | Silent | $n$ = 5 |
| N/A | Silent | $n$ = 6 |

**Table 1:** Activity states of V3 INs before and after neurochemical application.

| Active Neurons ($n$ = 11) | | |
|---|---|---|
| **VR Activity** | **Spinal Segment** | **Total Neurons** |
| *Tonic* | T8 - T13 | $n$ = 3 |
| | L1 - L4 | $n$ = 3 |
| *Rhythmic* | T1 -T7 | $n$ = 3 |
| *Slice* | T8 - T13 | $n$ = 1 |
| | L1 - L4 | $n$ = 1 |

**Table 2:** Regional location of active V3 INs after application of neurochemicals

Overall, these distinct responses support current evidence that V3 INs comprise multiple functional subtypes with distinct intrinsic properties and sensitivities to neuromodulators, consistent with prior findings (Borowska et al., 2013, 2015; Chopek et al., 2018a).

### 3.4 Rostro-Caudal Axis Reveals Variability in V3 IN Response

When comparing the response patterns of V3 INs across different spinal segments, their intrinsic properties at baseline and following neurochemical application revealed distinct regional trends. Comparisons were primarily focused between the caudal thoracic (T8–T13) and rostral lumbar (L1–L4) regions, as these consistently provided baseline data. However, the rostral thoracic (T1–T7) group was included for visualization purposes to illustrate how activity patterns in these more rostral neurons compared to caudal segments. RMP exhibited the greatest variability among all parameters, with caudal thoracic neurons showing the most stable membrane potentials between baseline and post-drug application. In contrast, rostral lumbar neurons displayed greater variability, with an overall depolarizing trend following neurochemical exposure. Rheobase values showed modest segmental differences, with a slight reduction post-drug application in the mid-thoracic region, whereas lumbar neurons exhibited slightly more hyperpolarized properties. FF was generally higher in mid-thoracic neurons compared to both upper thoracic and lumbar groups following neurochemical exposure, with minimal mean changes relative to baseline. $R_{in}$ displayed substantial variability across all segments, though a general decrease was observed post-drug application, particularly in the lumbar region, indicating possible shunting effects despite depolarization. Collectively, these results highlight segment-specific differences in baseline excitability and neurochemical responsiveness of V3 INs along the rostro-caudal axis of the spinal cord.

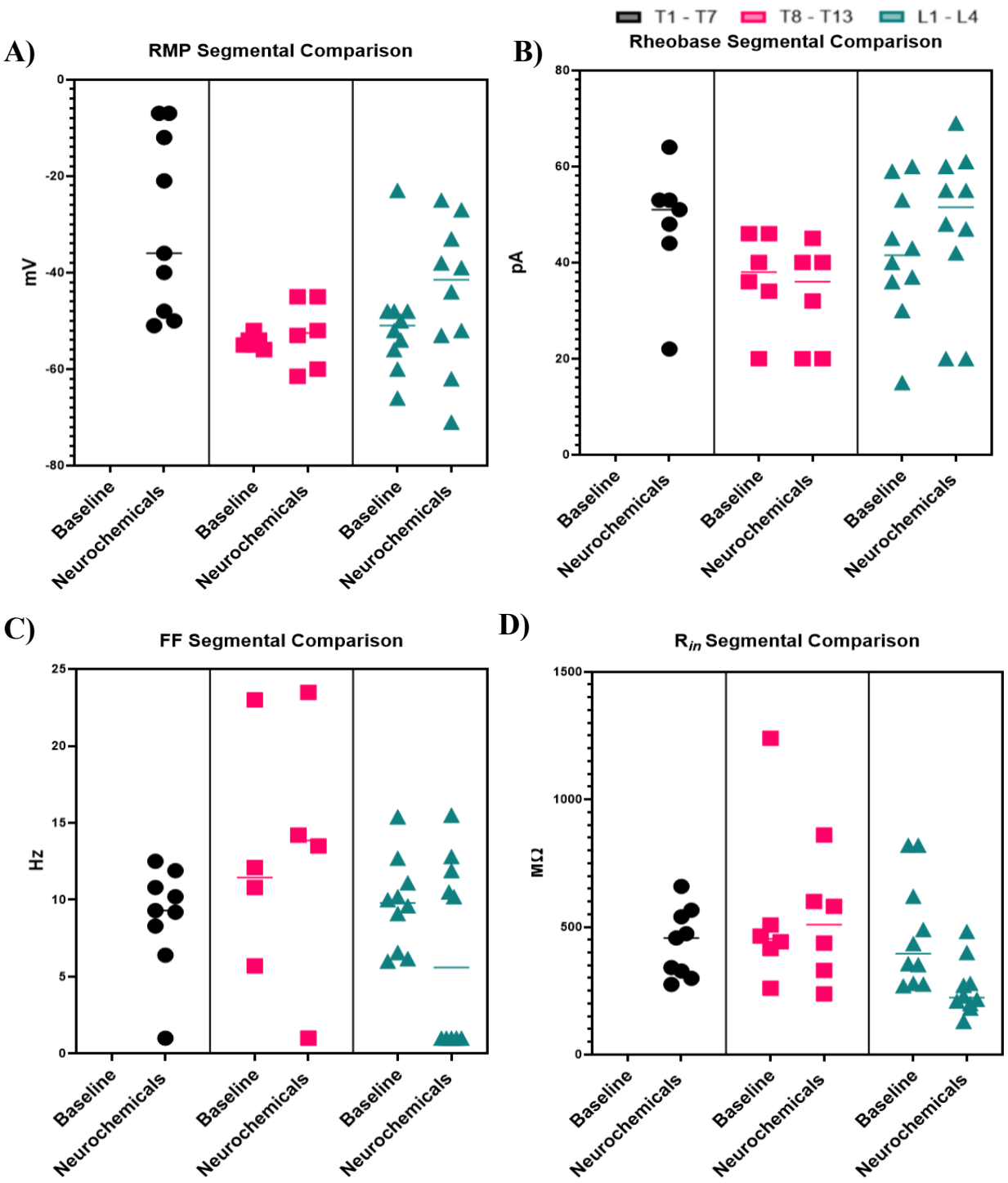


**Figure 19.** Response patterns of V3 INs across spinal segments under baseline conditions and following neurochemical application. Box plots represent variability within each segment T1 – T7 (black, $n = 9$), T8 – T13 (pink, $n = 6$), and L1 – L4 (teal, $n = 10$) showing segment-specific differences in RMP (A), rheobase (B), FF (C) and $R_{in}$ (D) from baseline to post neurochemical application.

### 3.5 Neurochemical Application Produces Variable Effects of Hyperpolarization-Dependant Properties of V3 INs

Among all analyzed neurons, baseline and post neurochemical application measurements of the amplitude of the hyperpolarization sag response and PIR response were only recorded in 15 of the 27 total neurons. Overall, V3 INs exhibited a slight overall depolarization in RMP following neurochemical exposure, though individual responses were highly variable. While subsets of neurons displayed modest increases in sag amplitude ($n$ = 5), the majority showed reduced amplitudes ($n$ = 10, **Figure 20, A**), suggesting that activation of serotonergic and NMDA-dependent conductances may influence the contribution of Ih currents (with sag measured from a fixed holding potential of −60 mV). When grouped by spinal segment, sag amplitude remained relatively consistent across thoracic and lumbar regions, with no significant segmental bias in post-drug responsiveness (**Figure 20, B**). Potentially indicating that the influence of neurochemicals on Ih-mediated depolarizing sag currents is broadly distributed across V3 populations rather than region-specific.

In contrast, PIR amplitude responses, quantified as the peak depolarization following release from the hyperpolarizing current steps (**Figure 11**), were more variable (**Figure 20, C**). While several neurons displayed enhanced rebound amplitudes ($n$ = 5), a comparable proportion exhibited substantial reductions or complete loss of PIR response ($n$ = 8), indicating distinct modulation patterns in rebound excitability within the population. Segmental comparisons revealed that rostral thoracic neurons displayed a general reduction in PIR amplitude following drug exposure, with 5/7 neurons failing to produce an action potential during the PIR response post neurochemical application. Whereas caudal thoracic and rostral lumbar neurons predominantly maintained PIR potentials (**Figure 21, D**), with only a single neuron in each region

transitioning from a detectable rebound at baseline to an absence of response after neurochemical application. This pattern suggests that rostral thoracic V3 INs may experience stronger shunting effects or altered calcium-dependent rebound mechanisms under neuromodulatory influence, while lumbar V3s retain greater rebound capacity, potentially reflecting their more prominent role in rhythmogenic drive.

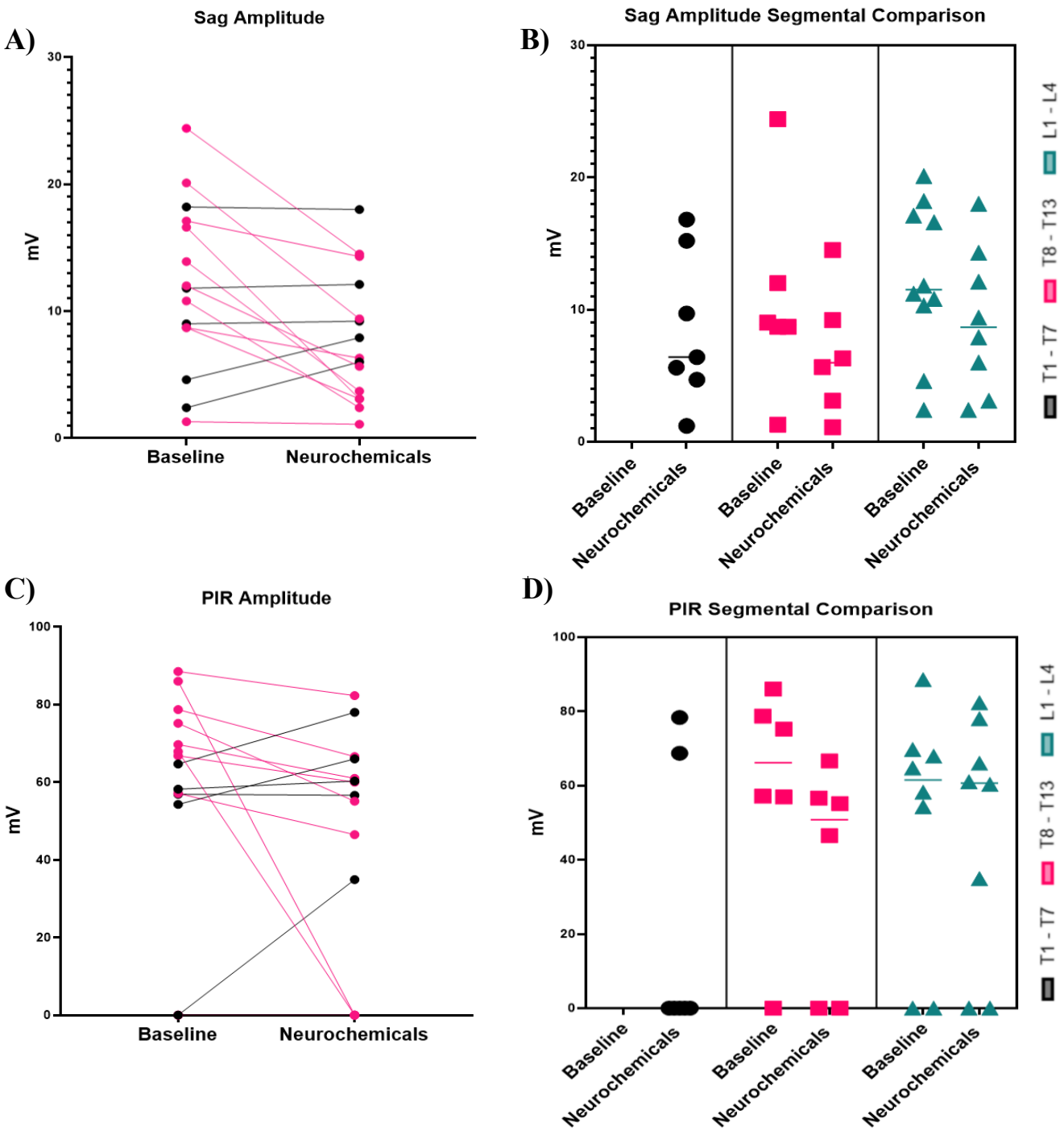


**Figure 20.** Sag and PIR amplitudes of V3 INs before and after neurochemical application. A) Paired data showing individual V3 IN hyperpolarizing sag response ($n$ = 15) to a hyperpolarizing current. B & D) Segmental comparisons of sag amplitude and PIR response across rostral thoracic (black, $n$ = 7), caudal thoracic (pink, $n$ = 6), and rostral lumbar (teal, $n$ = 8) segments. C) Paired data showing individual V3 IN PIR response ($n$ = 15) to a hyperpolarizing current. Neurons lacking a response are not included in this chart ($n$ = 2).

### 3.6 V3 INs Firing Pattern Following Neurochemical Application in Slice

In all recorded V3 INs that displayed activity following the application of neurochemicals, firing was not clearly related to ongoing VR activity. Neurons failed to show phase-related spiking or episodic bursts. We only managed to record from caudal thoracic and rostral lumbar V3 INs (**Figure 21**). Those in the rostral lumbar region were more likely to display a strong and consistent spike amplitude and frequency, while those in the caudal thoracic region were more likely to display more variable firing frequencies, however we still considered this to be tonic or non-rhythmic activity, as it was too irregular to be related to VR activity.

**A) Rostral thoracic V3 IN**

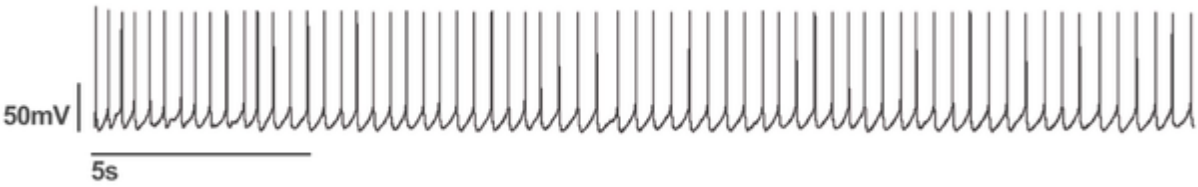


**B) Caudal thoracic V3 IN**

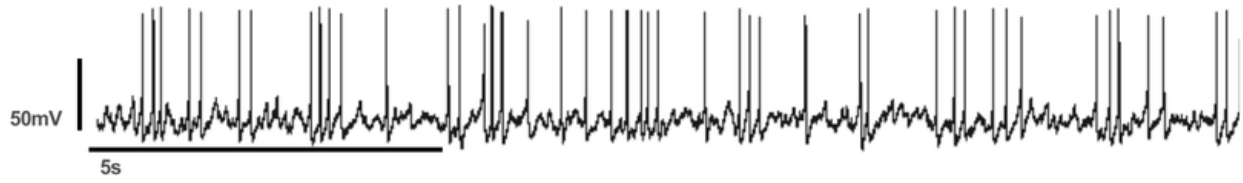


**Figure 21.** Whole-cell recordings reveal tonic firing patterns of V3 INs in slice preparation following neurochemical application. **A)** Current-clamp recording of a rostral lumbar V3 IN displaying tonic firing patterns. **B)** Current-clamp recording of a caudal thoracic V3 IN displaying tonic firing patterns.

### 3.7 V3 INs Firing Pattern During Tonic VR Activity in Dorsal Horn-Removed Preparation

Consistent with tonic activity patterns observed during rhythmic VR activity in the thoracic exposed preparation, V3 INs recorded in the dorsal horn-removed preparations also exhibited sustained tonic firing patterns in response to application of neurochemicals ($n$ = 7, **Figure 22**). Despite the absence of coordinated rhythmic activity, V3 INs remained depolarized and displayed continuous spiking, although at a lower frequency than observed in the thoracic exposed preparation. This suggests that tonic firing is maintained through intrinsic membrane properties and excitatory synaptic inputs within the ventral network that persist independent of sensory feedback.

**A) Rostral thoracic V3 during tonic VR activity**

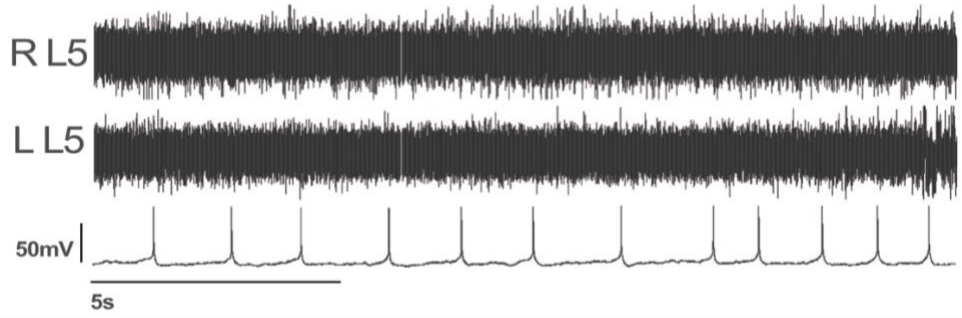


**B) Caudal thoracic V3 during tonic VR activity**

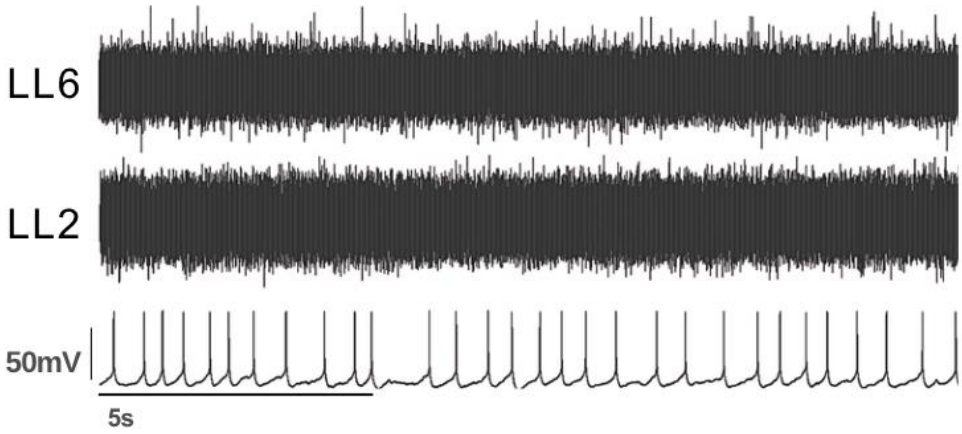


**C) Caudal lumbar V3 during tonic VR activity**

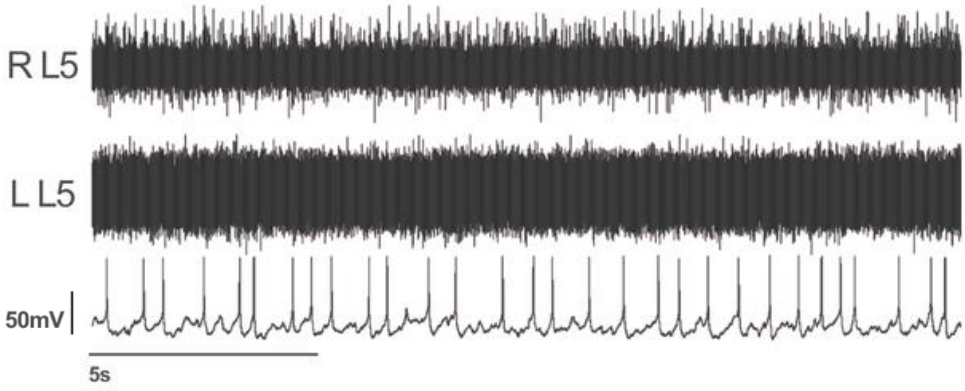


**Figure 22.** Whole-cell recordings reveal tonic firing patterns of V3 INs in dorsal horn-removed tonic preparation. Current-clamp recordings of a V3 IN located in the **A)** rostral and **B)** caudal thoracic as well as **C)** caudal lumbar regions showing tonic VR output.

### 3.8 V3 INs Firing Patterns During Rhythmic VR Activity

Some V3 INs recorded during rhythmic VR activity exhibited tonic firing patterns ($n$ = 8, **Figure 23**). Neurons recorded from these preparations lacked baseline recordings as rhythmic activity was induced prior to whole-cell access. Under current-clamp configuration, some V3 INs displayed continuously trains of action potentials throughout the rhythmic locomotor-like cycle (n = 3) rather than displaying phase-related or rhythmically modulated spiking. The remaining neurons ($n$ = 6 ) remained silent, with no spiking or action potentials.

## A) Rostral thoracic V3 during rhythmic VR activity

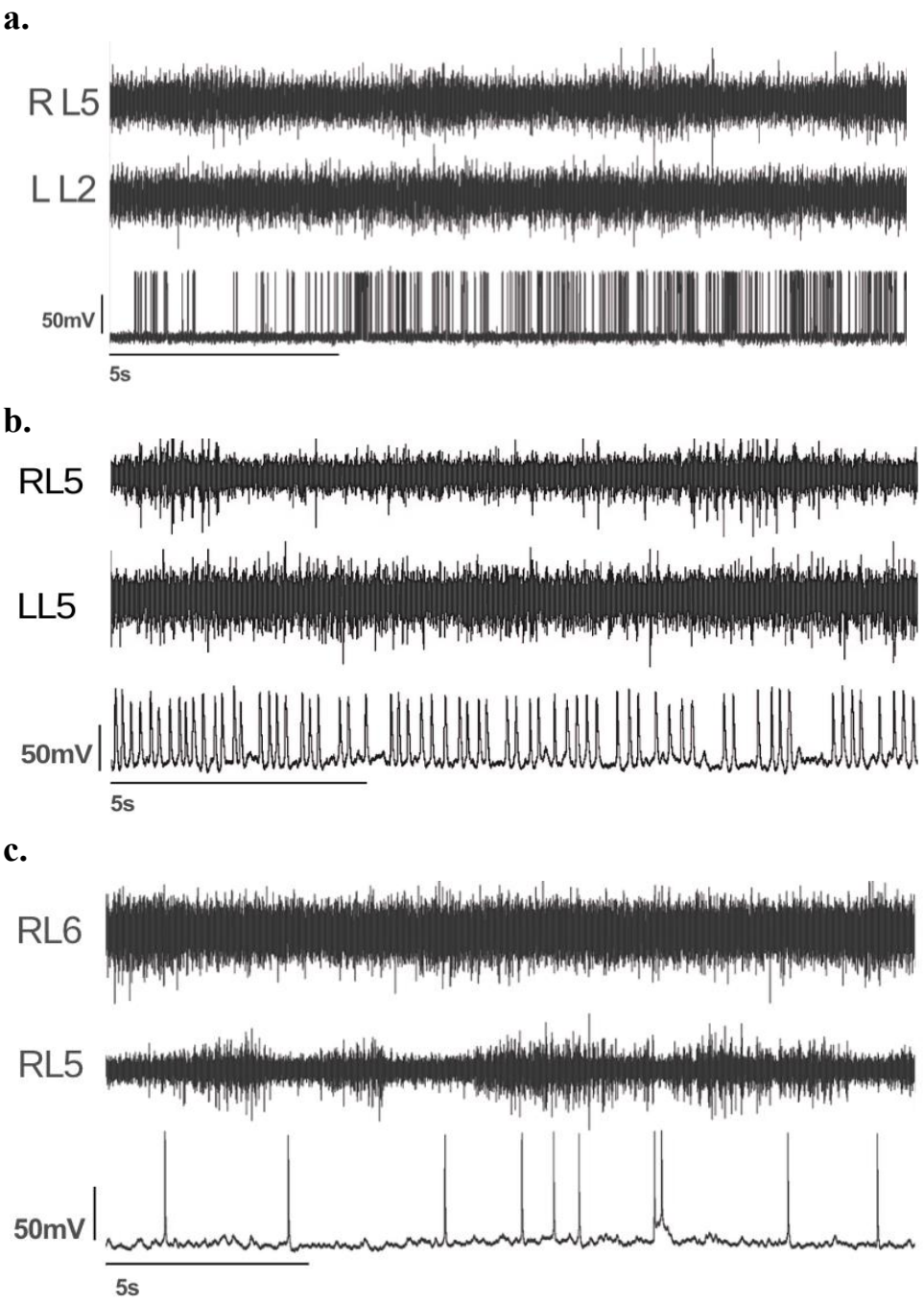


**Figure 23.** Intracellular current-clamp recordings with associated VR activity. **A)** Rhythmic VR output from **a.** right (R L5) and left (L L5) **b.** right (R L5) and left (L L2), and **c.** right (L L5) and left (L L5) roots with intracellular recordings of a V3 IN located in rostral thoracic segment displaying tonic firing throughout alternating VR bursts.

# Chapter IV: Discussion

## 4.1 Summary of Findings

The present study provides new insight into the electrophysiological behavior and activity patterns of genetically identified V3 INs within the neonatal mouse spinal cord during neurochemically induced rhythmic and tonic VR activity. Using WCPC recordings in conjunction with VR activity, this study provides the first detailed electrophysiological characterization of V3 INs during locomotor-like activity, partially addressing the existing gap in direct empirical evidence of their functional properties. By characterizing their intrinsic firing patterns under neurochemically induced fictive locomotor-like conditions in slice ($n$ = 5), thoracic exposed ($n$ = 12) and dorsal horn-removed ($n$ = 10) preparations, this work revealed that their activity and responses are diverse.

Across preparations, V3 INs exhibited distinct changes in excitability following application of 5-HT, NMDA, and DA. Responses ranged for each measure of excitability, from membrane depolarization and enhanced firing frequency to complete loss of repetitive firing and reduced input resistance. This diversity supports the previously established presence of functionally distinct subpopulations of V3 (Borowska et al., 2013, 2015; Chopek et al., 2018a). During both rhythmic and tonic VR activity, V3 INs displayed sustained tonic firing rather than phase-related oscillations, which paradoxically may still be consistent with their proposed role in stabilizing motor output during the step cycle (Danner et al., 2019). This idea is supported by previous work suggesting V3 INs contribute to the robustness and adaptability of the locomotor CPG by providing distributed excitatory drive across their functionally diverse subpopulations (Zhang et al., 2008; H. Zhang et al., 2025). Together, these findings expand on and support previous observations by demonstrating that distinct V3 subpopulations may have distinct

responses to serotonergic, dopaminergic and glutamatergic modulation during either tonic or rhythmic locomotor activity.

### 4.2 Development of Methods

To investigate the activity patterns of V3 INs during rhythmic VR activity, we utilized an *in vitro* spinal cord preparation of a neonatal mouse (P0 – P7). The use of a younger pup extended the viability of the preparation, as older spinal cords are larger, limiting oxygen diffusion and leading to rapid cellular deterioration and death. Additionally, pups older than P7 – P14 usually exhibit restrictions to their neuronal somas due to age related changes in their extracellular matrix and perineuronal sheaths (Husch et al., 2011). After experiencing little success in preparations > P5, subsequent experiments were conducted primarily on P0-P4.

Initial experiments using a thoracic-exposed preparation were largely unsuccessful due to factors such as the older age of pups, limited visual access, and developing technical proficiency. To improve soma access, we transitioned to a dorsal horn–removed preparation, as used in other studies (Dougherty et al., 2013c). Although this configuration provided improved visualization and access, rhythmic VR bursting was not reliably evoked ($n$ = 0/38). We therefore reverted to the thoracic-exposed preparation, by which point technical proficiency had improved and a more effective neurochemical cocktail had been developed, resulting in greater experimental success in evoking fictive locomotor-like activity.

### 4.3 Variable Intrinsic Excitability Responses May Reflect Functionally Distinct V3 INs Subpopulations

The present findings reveal that V3 INs exhibit distinct and variable responses to locomotor-inducing neurochemicals, reflecting distinct functional subtypes within this genetically defined population (Borowska et al., 2013). After application of 5-HT, NMDA, and DA, some

neurons depolarized and increased their firing frequency, whereas others hyperpolarized and became completely silent. These seemingly opposing and wide-ranging responses in intrinsic excitability responses to drug application, including RMP, rheobase, and $R_{in}$ suggest that V3 INs are not a uniform group of excitatory commissural neurons, but rather encompass multiple physiologically specialized subtypes. This variability aligns with previous anatomical and electrophysiological evidence (Blacklaws et al., 2015; Borowska et al., 2013, 2015; Chopek et al., 2018a; Deska-Gauthier et al., 2024) suggesting that V3 populations distributed across the rostro-caudal axis and ventral, intermediate and dorsal spinal regions differ in their synaptic inputs, projection targets, and intrinsic properties.

The diverse electrophysiological responses observed across spinal segments highlight the variability of V3 INs and support the existence of functionally specialized subpopulations along the rostro caudal axis. V3 neurons within the rostral lumbar region, corresponding to one of the rhythmogenic cores of the locomotor CPG in rodents (Cowley & Schmidt, 1997; Kiehn & Kjaerulff, 1998; Kjaerulff & Kiehn, 1996), exhibited greater sensitivity to neurochemical modulation. This aligns with previous findings showing that rostral spinal segments (T13/L1 – L2) contain a 5-HT-sensitive distributed network that promote intrinsic bursting and oscillatory behaviour (Cowley & Schmidt, 1997; Kiehn, 2006). The caudal lumbar V3 INs in this study therefore displayed physiological characteristics consistent with their observed role in maintaining a stable and robust locomotor output by providing excitatory drive to contralateral rhythm-generating circuits (Rybak et al., 2015; Zhang et al., 2008). In contrast, thoracic V3 neurons remained comparatively stable in responses to intrinsic measures, showing minimal changes in RMP, rheobase, $R_{in}$, FF, which may support prior evidence that thoracic neurons function as excitatory distribution or relay elements that integrate and transmit locomotor drive between

rhythmogenic centers rather than generating rhythmic bursts themselves (Danner et al., 2017; Laliberte et al., 2019).

Collectively, the various responses of V3 INs observed in this study highlight their multifunctional role within the central pattern generator, acting not as a single excitatory contributor but as distributed network components capable of balancing excitation, stabilization, and modulation of rhythmic motor output. The coexistence of these distinct electrophysiological profiles supports the pre-existing assumption that V3 circuits flexibly shape locomotor output across different speeds and behavioral contexts, supporting both hind and forelimb coordination (thoracic V3 INs) and adaptive gait modulation (lumbar V3 INs) (Laliberte et al., 2019; H. Zhang et al., 2022; Zhong et al., 2006)

**4.4 Interpreting the Effects of Neurochemical Application on V3 INs**

It has been well documented that NMDA, 5-HT and DA produce rhythmic VR activity in the rodent spinal cord (Cazalets et al., 1990, 1992; Chacon et al., 2023; Cheng et al., 2019; Cowley & Schmidt, 1994, 1995, 1997; Hernandez et al., 1991). However, when using exogenous neurochemicals to evoke an intrinsically generated behavior, it is important to consider their individual actions on the target neurons; in this case, V3 INs. The effects of 5-HT on spinal neurons vary according to receptor subtype distribution, particularly among 5-$HT_2$A and 5-$HT_7$ (excitatory) and 5-$HT_1$A (inhibitory) receptors, which play essential roles in descending activation and modulation of locomotor networks (Liu & Jordan, 2005). In most spinal CINs, 5-HT increases excitability by depolarizing the RMP and elevating $R_{in}$ (Abbinanti et al., 2012; Abbinanti & Harris-Warrick, 2012), therefor enhancing neuronal firing during locomotion. In contrast, recent findings suggest that 5-HT's influence on V3 INs is more heterogeneous: while some neurons exhibit increased excitability, others show decreased or unchanged responses following 5-HT application

(Zaman, 2024), reflecting the functional diversity and variable 5-HT receptor expression within this population. These findings support the concept that 5HT may act at multiple levels and in multiple ways to alter the gain in either sensory afferent-induced or ongoing intrinsic rhythm generation, depending upon environmental or experimental conditions.

In contrast, the intrinsic response patterns of V3 INs to isolated NMDA exposure have not been characterized. Although NMDA has been used in locomotor-inducing protocols involving V3 INs (Borowska et al., 2013; Danner et al., 2019; Zhang et al., 2008), it has primarily been by activating the broader locomotor network rather than to examine its direct cellular effects on V3 INs. Although these experiments were not performed specifically in V3 INs, NMDA application has been shown to have a variable effects in both ascending and descending CINs in the neonatal rat spinal cord (Cheng et al., 2019), including depolarization of RMP and reductions in $R_{in}$.

Among all neurons that exhibited reductions in $R_{in}$, the magnitude of change varied widely, ranging from 8% to 83% (mean decrease ≈ 42%). Nearly half of these neurons showed reductions greater than 50%, indicating substantial increases in membrane conductance. This widespread decrease in Rin is consistent with activation of tonic excitatory and inhibitory conductances, such as NMDA and 5-$HT_{1A}$ receptor-mediated currents, which can depolarize the membrane while concurrently shunting synaptic and injected currents (Cheng et al., 2019).

In the present study, 8 of the 17 neurons with pre- and post-neurochemical recordings exhibited membrane depolarization accompanied by reduced $R_{in}$ relative to baseline recordings. These neurons were in the rostral lumbar ($n$ = 5) and caudal thoracic ($n$ = 3) segments. Given NMDA's established role in generating rhythmic bursting and plateau potentials in other spinal neurons (Hochman et al., 1994; Kiehn & Kjaerulff, 1998; MacLean et al., 1997), the present findings provide the first evidence suggesting that a sub population of V3 INs may enter a high-

conductance, depolarized state following combined NMDA/5-HT exposure. Characterized by membrane depolarization and reduced input resistance, these physiological changes are consistent with strong synaptic recruitment during network activation (Destexhe et al., 2003; Hochman et al., 1994; Raastad et al., 1998), potentially representing the ventral V3 population (Borowska et al., 2013; H. Zhang et al., 2025) that are known for their role in distributing excitation within the locomotor CPG (Zhang et al., 2008).

Interestingly, a small subset of V3 INs exhibited hyperpolarization and decreased input resistance following neurochemical application ($n$ = 7/16), with a small subgroup also exhibiting PIR responses ($n$ = 4). Given that V3 are excitatory, glutamatergic INs, this pattern likely arises through a combination of network inhibition and intrinsic membrane mechanisms. However, because the membrane receptor profile of V3 INs remains incompletely characterized, these responses may also reflect direct activation of inhibitory or outward-current–generating conductances on V3 membranes, rather than solely network-mediated inhibition. During NMDA/5-HT exposure, recruitment of inhibitory INs can impose tonic $GABA_A$/glycinergic conductances on some V3 INs (Lin et al., 2023), producing a shunting hyperpolarization (Goulding, 2009b; Kiehn & Kjaerulff, 1998). In addition, activation of 5-$HT_1$A receptors or $Ca^{2+}$-dependent $K^+$ channels can generate outward currents that lower Rin (Liu & Jordan, 2005; Raastad et al., 1998). These neurons may therefore represent dorsal or intermediate V3 IN subtypes with stronger inhibitory receptor expression or adaptive outward conductances. Functionally, this subpopulation could serve as stabilizing or gain-control elements that dampen excessive excitation within the commissural network during locomotor activation.

### 4.5 V3 INs Exhibit Non-Rhythmic Firing During Tonic VR Activity

Neurons were recorded during tonic VR activity ($n$ = 13), of which only 7 displayed active firing. Neurons were in the rostral ($n$ = 1) and caudal ($n$ = 3) thoracic, as well as rostral lumbar (n = 3) segments. Following neurochemical application, V3 INs exhibited sustained tonic firing in current-clamp recordings, consistent with their depolarized and high-conductance membrane state described above. The persistence of tonic discharge, even in the absence of rhythmic VR output, suggests that these neurons are intrinsically capable of maintaining continuous excitatory drive when sufficiently depolarized. Such behavior is consistent with earlier findings showing that aCINs exhibit tonic firing during 5-HT/NMDA-evoked fictive locomotion (Zhong et al., 2006), Given that the lateral V3 IN population includes excitatory, bifurcating commissural interneurons (Chopek et al., 2018a), their tonic activity in our recordings may reflect a role in providing baseline excitatory drive within the locomotor network.

A subset of V3 INs ($n$ = 6) remained non-responsive to 5-HT/NMDA application, showing little or no change in intrinsic properties. This likely reflects underlying diversity in receptor expression and intrinsic excitability within the V3 IN population or may reflect contradictory responses to each of the neurochemicals applied in the absence of ongoing rhythmic activity. Some may lack sufficient densities of excitatory 5-$HT_{2A/7}$ or NMDA receptors or possess balancing inhibitory conductances that counteract depolarizing drive (Borowska et al., 2015; Liu & Jordan, 2005) Others may be positioned outside the rhythmogenic cores of the locomotor CPG and therefore receive limited synaptic recruitment under neurochemical activation, or may require ongoing rhythmic activity to enlist their activity (Cowley & Schmidt, 1997). Functionally, these non-responsive V3s may act as context-dependent relay or modulatory elements, becoming

engaged only under stronger or task-specific descending inputs rather than during pharmacologically induced locomotor states.

### 4.6 V3 INs Exhibit Tonic Firing Patterns During Rhythmic VR Activity

During rhythmic VR bursting most V3 INs displayed tonic firing patterns, rather than phase-related oscillatory discharge patterns ($n$ = 3). However, limited conclusions can be drawn from this limited sample, particularly given the lack of robust rhythmic VR activity recorded in these preparations (**Figure 23**). Nonetheless these non-rhythmic activity patterns could suggest that V3 INs provide a continuous excitatory input to the locomotor network rather than contributing directly to rhythm generation during locomotor-like activities. Such persistent activation could maintain a balanced level of excitatory drive across left–right and flexor–extensor centers, thereby stabilizing locomotor output throughout each cycle (Zhang et al., 2008; H. Zhang et al., 2025). Furthermore, the three neurons that were tonically active exhibited high (540 - 660 MΩ, mean = 588 MΩ) $R_{in}$, while the remining inactive neurons displayed low $R_{in}$ (470 – 270 MΩ, mean = 366 MΩ), potentially connecting the observation that neurons with higher input resistances have a greater likelihood of firing.

This interpretation aligns with computational and experimental work (Danner et al., 2019) which proposed that V3 INs mediate mutual excitation between contralateral extensor centers to promote symmetry and sustain rhythmic output. In that model, V3s do not initiate rhythmogenesis but instead ensure the robustness and balance of the rhythm produced by V2a and other rhythm-generating populations. Comparable tonic excitatory roles have also been described in zebrafish V3 neurons, which show steady, non-oscillatory firing during locomotor bouts and are thought to stabilize network output and coordinate left–right alternation (Wiggin et al., 2022).

The absence of phase-related activity in the present study therefore supports a modulatory rather than pacemaking role for V3 INs. Functionally, their persistent firing may act as a stabilizing 'scaffold' within the locomotor central pattern generator, sustaining depolarization in rhythmogenic INs and motor pools while preventing collapse of rhythmic drive during transitions or asymmetries in excitation. These findings refine the current model of the mammalian locomotor CPG by suggesting that V3 INs contribute to the amplification of supraspinal motor commands (H. Zhang et al., 2025); neurons that reinforce rhythm robustness and bilateral coordination rather than directly tuning locomotor bursts.

### 4.7 Limitations

Several limitations should be considered when interpreting the results of this study. First, the overall sample size was significantly smaller than originally intended. Challenges related to technical proficiency, equipment constraints, and the time required to optimize a new whole-cord preparation protocol limited the number of viable recordings obtained, resulting in the low overall viable preparations ($n$ = 27/214) A larger dataset would strengthen the significance of the current findings as well as improve overall generalizability.

Second, the age of the preparation represents an important physiological constraint. Recordings were obtained from neonatal tissue to improve preparation survival as well as improved visualization of neurons. However, the drawback of using neonates includes the intrinsic membrane properties, channel expression, and synaptic connectivity being immature. Spinal locomotor circuits in the neonatal mouse do not reach full electrophysiological and neuromodulatory maturity until well into postnatal development (P21) (Borowska et al., 2015). As a result, the firing properties and neurochemical responsiveness observed in this study may not

fully represent those observed in mature V3 IN. However, more mature preparations will have their own accessibility limitations associated with prep survival rate and visualization.

Third, there are limitations associated with the VR recordings. Because each VR contains a mixed population of flexor and extensor motor axons, tonic VR output may arise from the superimposition of multiple asynchronous rhythms, rather than representing a truly rhythmic underlying network state (Cowley and Schmidt 1994). Although VR recordings in these experiments were typically taken from L2 and L5, these effects should be minimized, since they are more likely to occur in VRs less directly associated with flexion/extension such as L3 and L6 (Cowley and Schmidt 1994), this is still a potential limitation. Additionally, the quality of the suction seal on the VR can influence signal clarity; a poor seal may obscure subtle rhythmicity and produce an artificially tonic appearance.

Finally, spatial constraints within the recording chamber with VRs suctioned restricted the segments of the cord that could be reliably accessed. The microscope objective, patch pipette angle, and placement of the suction electrodes often prevented simultaneous VR recording and patch-clamp access in rostral lumbar areas when using the dorsal-horn removed preparation. This reduced the diversity of segments during rhythmic VR activity sampled and may have biased the dataset toward neurons that were simply more accessible within the preparation (thoracic segments).

Together, these factors highlight the need for future work using larger sample sizes, more mature preparations are a possibility, and expanded spatial access to spinal segments to fully characterize the diversity of V3 INs responses during tonic and rhythmic VR activity in the neonatal mouse spinal cord.

# Chapter V: Conclusion

This study provides novel insight into the firing patterns and intrinsic properties of V3 INs during tonic and rhythmic VR activity. While the original hypothesis predicted that V3 INs would exhibit robust rhythmic firing during drug-induced locomotor-like activity, the present findings do not support this expectation. Instead, V3 INs predominantly displayed sustained, tonic firing across both tonic and rhythmic networks states, even when rhythmic VR output was present. However, due to our small sample size, more data collection and analysis need to be done prior to making any conclusive remarks.

While these results refine our understanding of how excitatory commissural pathways support locomotor stability, they also underscore how much remains unknown. Future work utilizing larger sample sizes and more mature preparations will be essential to determine whether distinct V3 subtypes contribute differently to extensor drive, interlimb coordination, or rhythm robustness. By establishing the first direct intracellular characterization of V3 IN firing patterns during locomotor-like activity, this study provides a foundational step toward unraveling the specific circuit roles of V3 INs within the mammalian central pattern generator.

# References


Abbinanti, M. D., & Harris-Warrick, R. M. (2012). Serotonin modulates multiple calcium current subtypes in commissural interneurons of the neonatal mouse. *Journal of Neurophysiology*, *107*(8), 2212–2219. https://doi.org/10.1152/jn.00768.2011

Abbinanti, M. D., Zhong, G., & Harris-Warrick, R. M. (2012). Postnatal emergence of serotonin-induced plateau potentials in commissural interneurons of the mouse spinal cord. *Journal of Neurophysiology*, *108*(8), 2191–2202. https://doi.org/10.1152/jn.00336.2012

Adrian, E. D., & Bronk, D. W. (1928). The discharge of impulses in motor nerve fibres. *The Journal of Physiology*, *66*(1), 81–101. https://doi.org/10.1113/jphysiol.1928.sp002509

Akay, T., Tourtellotte, W. G., Arber, S., & Jessell, T. M. (2014). Degradation of mouse locomotor pattern in the absence of proprioceptive sensory feedback. *Proceedings of the National Academy of Sciences*, *111*(47), 16877–16882. https://doi.org/10.1073/pnas.1419045111

Bakels, R., & Kernell, D. (1993). Average but not continuous speed match between motoneurons and muscle units of rat tibialis anterior. *Journal of Neurophysiology*, *70*(4), 1300–1306. https://doi.org/10.1152/jn.1993.70.4.1300

Barnes, N. M., & Sharp, T. (1999). A review of central 5-HT receptors and their function. *Neuropharmacology*, *38*(8), 1083–1152. https://doi.org/10.1016/S0028-3908(99)00010-6

Beato, M., & Nistri, A. (1999). Interaction Between Disinhibited Bursting and Fictive Locomotor Patterns in the Rat Isolated Spinal Cord. *Journal of Neurophysiology*, *82*(5), 2029–2038. https://doi.org/10.1152/jn.1999.82.5.2029

Bertran-Gonzalez, J., Bosch, C., Maroteaux, M., Matamales, M., Hervé, D., Valjent, E., & Girault, J.-A. (2008). Opposing Patterns of Signaling Activation in Dopamine D 1 and D 2 Receptor-Expressing Striatal Neurons in Response to Cocaine and Haloperidol. *The Journal of Neuroscience*, *28*(22), 5671–5685. https://doi.org/10.1523/JNEUROSCI.1039-08.2008

Blacklaws, J., Deska-Gauthier, D., Jones, C. T., Petracca, Y. L., Liu, M., Zhang, H., Fawcett, J. P., Glover, J. C., Lanuza, G. M., & Zhang, Y. (2015). Sim1 is required for the migration and axonal projections of V3 interneurons in the developing mouse spinal cord. *Developmental Neurobiology*, *75*(9), 1003–1017. https://doi.org/10.1002/dneu.22266

Bonnot, A., Whelan, P. J., Mentis, G. Z., & O'Donovan, M. J. (2002). Locomotor-like activity generated by the neonatal mouse spinal cord. *Brain Research Reviews*, *40*(1–3), 141–151. https://doi.org/10.1016/S0165-0173(02)00197-2

Borowska, J., Jones, C. T., Deska-Gauthier, D., & Zhang, Y. (2015). V3 interneuron subpopulations in the mouse spinal cord undergo distinctive postnatal maturation processes. *Neuroscience*, *295*, 221–228. https://doi.org/10.1016/j.neuroscience.2015.03.024

Borowska, J., Jones, C. T., Zhang, H., Blacklaws, J., Goulding, M., & Zhang, Y. (2013). Functional Subpopulations of V3 Interneurons in the Mature Mouse Spinal Cord. *The Journal of Neuroscience*, *33*(47), 18553–18565. https://doi.org/10.1523/JNEUROSCI.2005-13.2013

Briscoe, J., Pierani, A., Jessell, T. M., & Ericson, J. (2000). A Homeodomain Protein Code Specifies Progenitor Cell Identity and Neuronal Fate in the Ventral Neural Tube. *Cell*, *101*(4), 435–445. https://doi.org/10.1016/S0092-8674(00)80853-3

Brock, L. G., Coombs, J. S., & Eccles, J. C. (1952). The recording of potentials from motoneurones with an intracellular electrode. *The Journal of Physiology*, *117*(4), 431–460. https://doi.org/10.1113/jphysiol.1952.sp004759

Brodin, L., Grillner, S., & Rovainen, C. M. (1985). N-methyl-d-aspartate (NMDA), kainate and quisqualate receptors and the generation of fictive locomotion in the lamprey spinal cord. *Brain Research*, *325*(1–2), 302–306. https://doi.org/10.1016/0006-8993(85)90328-2

Brown, T. G. (1911). The intrinsic factors in the act of progression in the mammal. *Proceedings of the Royal Society of London. Series B, Containing Papers of a Biological Character*, *84*(572), 308–319. https://doi.org/10.1098/rspb.1911.0077

Brown, T. G. (1914). On the nature of the fundamental activity of the nervous centres; together with an analysis of the conditioning of rhythmic activity in progression, and a theory of the evolution of function in the nervous system. *The Journal of Physiology*, *48*(1), 18–46. https://doi.org/10.1113/jphysiol.1914.sp001646

Buchanan, J. T. (2001). Contributions of identifiable neurons and neuron classes to lamprey vertebrate neurobiology. *Progress in Neurobiology*, *63*(4), 441–466. https://doi.org/10.1016/S0301-0082(00)00050-2

Buchanan, J. T., & Grillner, S. (1987). Newly Identified 'Glutamate Interneurons' and Their Role in Locomotion in the Lamprey Spinal Cord. *Science*, *236*(4799), 312–314. https://doi.org/10.1126/science.3563512

Carter, M. C., & Smith, J. L. (1986). Simultaneous control of two rhythmical behaviors. I. Locomotion with paw-shake response in normal cat. *Journal of Neurophysiology*, *56*(1), 171–183. https://doi.org/10.1152/jn.1986.56.1.171

Cazalets, J. R., Grillner, P., Menard, I., Cremieux, J., & Clarac, F. (1990). Two types of motor rhythm induced by NMDA and amines in an in vitro spinal cord preparation of neonatal rat. *Neuroscience Letters*, *111*(1–2), 116–121. https://doi.org/10.1016/0304-3940(90)90354-C

Cazalets, J. R., Sqalli-Houssaini, Y., & Clarac, F. (1992). Activation of the central pattern generators for locomotion by serotonin and excitatory amino acids in neonatal rat. *The Journal of Physiology*, *455*(1), 187–204. https://doi.org/10.1113/jphysiol.1992.sp019296

Chacon, C., Nwachukwu, C. V., Shahsavani, N., Cowley, K. C., & Chopek, J. W. (2023). Lumbar V3 interneurons provide direct excitatory synaptic input onto thoracic sympathetic preganglionic neurons, linking locomotor, and autonomic spinal systems. *Frontiers in Neural Circuits*, *17*. https://doi.org/10.3389/fncir.2023.1235181

Cheng, Y., Ge, R., Chen, K., & Dai, Y. (2019). Modulation of NMDA-mediated intrinsic membrane properties of ascending commissural interneurons in neonatal rat spinal cord. *Journal of Integrative Neuroscience*, *18*(2). https://doi.org/10.31083/j.jin.2019.02.129

Chopek, J. W., Nascimento, F., Beato, M., Brownstone, R. M., & Zhang, Y. (2018a). Sub-populations of Spinal V3 Interneurons Form Focal Modules of Layered Pre-motor Microcircuits. *Cell Reports*, *25*(1), 146-156.e3. https://doi.org/10.1016/j.celrep.2018.08.095

Chopek, J. W., Nascimento, F., Beato, M., Brownstone, R. M., & Zhang, Y. (2018b). Sub-populations of Spinal V3 Interneurons Form Focal Modules of Layered Pre-motor Microcircuits. *Cell Reports*, *25*(1), 146-156.e3. https://doi.org/10.1016/j.celrep.2018.08.095

Cohen, A. H., & Wallen, P. (1980). The neuronal correlate of locomotion in fish. *Experimental Brain Research*, *41*(1). https://doi.org/10.1007/BF00236674

Cohen, L. A., & Cohen, M. L. (1956). Arthrokinetic Reflex of the Knee. *American Journal of Physiology-Legacy Content*, *184*(2), 433–437. https://doi.org/10.1152/ajplegacy.1956.184.2.433

Conway, B. A., Hultborn, H., & Kiehn, O. (1987). Proprioceptive input resets central locomotor rhythm in the spinal cat. *Experimental Brain Research*, *68*(3). https://doi.org/10.1007/BF00249807

Cowley, K. C., & Schmidt, B. J. (1994). A comparison of motor patterns induced by , acetylcholine and serotonin in the in vitro neonatal rat spinal cord. *Neuroscience Letters*, *171*(1–2), 147–150. https://doi.org/10.1016/0304-3940(94)90626-2

Cowley, K. C., & Schmidt, B. J. (1995). Effects of inhibitory amino acid antagonists on reciprocal inhibitory interactions during rhythmic motor activity in the in vitro neonatal rat spinal cord. *Journal of Neurophysiology*, *74*(3), 1109–1117. https://doi.org/10.1152/jn.1995.74.3.1109

Cowley, K. C., & Schmidt, B. J. (1997). Regional Distribution of the Locomotor Pattern-Generating Network in the Neonatal Rat Spinal Cord. *Journal of Neurophysiology*, *77*(1), 247–259. https://doi.org/10.1152/jn.1997.77.1.247

Danner, S. M., Shevtsova, N. A., Frigon, A., & Rybak, I. A. (2017). Computational modeling of spinal circuits controlling limb coordination and gaits in quadrupeds. *ELife*, *6*. https://doi.org/10.7554/eLife.31050

Danner, S. M., Zhang, H., Shevtsova, N. A., Borowska-Fielding, J., Deska-Gauthier, D., Rybak, I. A., & Zhang, Y. (2019). Spinal V3 Interneurons and Left–Right Coordination in Mammalian Locomotion. *Frontiers in Cellular Neuroscience*, *13*. https://doi.org/10.3389/fncel.2019.00516

Delvolvé, I., Bem, T., & Cabelguen, J.-M. (1997). Epaxial and Limb Muscle Activity During Swimming and Terrestrial Stepping in the Adult Newt, *Pleurodeles waltl*. *Journal of Neurophysiology*, *78*(2), 638–650. https://doi.org/10.1152/jn.1997.78.2.638

Derderian, C., Shumway, K., & Tadi, P. (2023). Physiology, Withdrawal Response. *StatsPearl*. https://www.ncbi.nlm.nih.gov/books/NBK544292/

Deska-Gauthier, D., Borowska-Fielding, J., Jones, C., Zhang, H., MacKay, C. S., Michail, R., Bennett, L. A., Bikoff, J. B., & Zhang, Y. (2024). Embryonic temporal-spatial delineation of excitatory spinal V3 interneuron diversity. *Cell Reports*, *43*(1), 113635. https://doi.org/10.1016/j.celrep.2023.113635

Deska-Gauthier, D., & Zhang, Y. (2019). The functional diversity of spinal interneurons and locomotor control. *Current Opinion in Physiology*, *8*, 99–108. https://doi.org/10.1016/j.cophys.2019.01.005

Destexhe, A., Rudolph, M., & Paré, D. (2003). The high-conductance state of neocortical neurons in vivo. *Nature Reviews Neuroscience*, *4*(9), 739–751. https://doi.org/10.1038/nrn1198

Dougherty, K. J. (2023). Distinguishing subtypes of spinal locomotor neurons to inform circuit function and dysfunction. *Current Opinion in Neurobiology*, *82*, 102763. https://doi.org/10.1016/j.conb.2023.102763

Dougherty, K. J., & Ha, N. T. (2019). The rhythm section: an update on spinal interneurons setting the beat for mammalian locomotion. *Current Opinion in Physiology*, *8*, 84–93. https://doi.org/10.1016/j.cophys.2019.01.004

Dougherty, K. J., & Kiehn, O. (2010). Firing and Cellular Properties of V2a Interneurons in the Rodent Spinal Cord. *The Journal of Neuroscience*, *30*(1), 24–37. https://doi.org/10.1523/JNEUROSCI.4821-09.2010

Dougherty, K. J., Zagoraiou, L., Satoh, D., Rozani, I., Doobar, S., Arber, S., Jessell, T. M., & Kiehn, O. (2013a). Locomotor Rhythm Generation Linked to the Output of Spinal Shox2 Excitatory Interneurons. *Neuron*, *80*(4), 920–933. https://doi.org/10.1016/j.neuron.2013.08.015

Dougherty, K. J., Zagoraiou, L., Satoh, D., Rozani, I., Doobar, S., Arber, S., Jessell, T. M., & Kiehn, O. (2013b). Locomotor Rhythm Generation Linked to the Output of Spinal Shox2 Excitatory Interneurons. *Neuron*, *80*(4), 920–933. https://doi.org/10.1016/j.neuron.2013.08.015

Dougherty, K. J., Zagoraiou, L., Satoh, D., Rozani, I., Doobar, S., Arber, S., Jessell, T. M., & Kiehn, O. (2013c). Locomotor Rhythm Generation Linked to the Output of Spinal Shox2 Excitatory Interneurons. *Neuron*, *80*(4), 920–933. https://doi.org/10.1016/j.neuron.2013.08.015

Duysens, J., & Pearson, K. G. (1980). Inhibition of flexor burst generation by loading ankle extensor muscles in walking cats. *Brain Research*, *187*(2), 321–332. https://doi.org/10.1016/0006-8993(80)90206-1

Duysens, J., & Van de Crommert, H. W. A. A. (1998). Neural control of locomotion; Part 1: The central pattern generator from cats to humans. *Gait & Posture*, *7*(2), 131–141. https://doi.org/10.1016/S0966-6362(97)00042-8

Eccles, J. C., Fatt, P., & Koketsu, K. (1954). Cholinergic and inhibitory synapses in a pathway from motor-axon collaterals to motoneurones. *The Journal of Physiology*, *126*(3), 524–562. https://doi.org/10.1113/jphysiol.1954.sp005226

Engberg, I., & Lundberg, A. (1969). An Electromyographic Analysis of Muscular Activity in the Hindlimb of the Cat during Unrestrained Locomotion. *Acta Physiologica Scandinavica*, *75*(4), 614–630. https://doi.org/10.1111/j.1748-1716.1969.tb04415.x

Falgairolle, M., & O'Donovan, M. J. (2021). Optogenetic Activation of V1 Interneurons Reveals the Multimodality of Spinal Locomotor Networks in the Neonatal Mouse. *The Journal of Neuroscience*, *41*(41), 8545–8561. https://doi.org/10.1523/JNEUROSCI.0875-21.2021

Flaive, A., Fougère, M., van der Zouwen, C. I., & Ryczko, D. (2020). Serotonergic Modulation of Locomotor Activity From Basal Vertebrates to Mammals. *Frontiers in Neural Circuits*, *14*. https://doi.org/10.3389/fncir.2020.590299

Forssberg, H. (1979). Stumbling corrective reaction: a phase-dependent compensatory reaction during locomotion. *Journal of Neurophysiology*, *42*(4), 936–953. https://doi.org/10.1152/jn.1979.42.4.936

Forssberg, H., & Grillner, S. (1973). The locomotion of the acute spinal cat injected with clonidine i.v. *Brain Research*, *50*(1), 184–186. https://doi.org/10.1016/0006-8993(73)90606-9

Frolich, L. M., & Biewener, A. A. (1992). Kinematic and Electromyographic Analysis of the Functional Role of the Body Axis During Terrestrial and Aquatic Locomotion in the Salamander *Ambystoma Tigrinum*. *Journal of Experimental Biology*, *162*(1), 107–130. https://doi.org/10.1242/jeb.162.1.107

Fu, C., Cao, Z.-D., & Fu, S.-J. (2019). Predation experience underlies the relationship between locomotion capability and survival. *Comparative Biochemistry and Physiology Part A: Molecular & Integrative Physiology*, *227*, 32–38. https://doi.org/10.1016/j.cbpa.2018.09.005

Gosgnach, S., Lanuza, G. M., Butt, S. J. B., Saueressig, H., Zhang, Y., Velasquez, T., Riethmacher, D., Callaway, E. M., Kiehn, O., & Goulding, M. (2006). V1 spinal neurons regulate the speed of vertebrate locomotor outputs. *Nature*, *440*(7081), 215–219. https://doi.org/10.1038/nature04545

Goulding, M. (2009a). Circuits controlling vertebrate locomotion: moving in a new direction. *Nature Reviews Neuroscience*, *10*(7), 507–518. https://doi.org/10.1038/nrn2608

Goulding, M. (2009b). Circuits controlling vertebrate locomotion: moving in a new direction. *Nature Reviews Neuroscience*, *10*(7), 507–518. https://doi.org/10.1038/nrn2608

Granit, R., KernellL, D., & Shortess, G. K. (1963). Quantitative Aspects of Repetative Firing of Mammalian Motoneurons, Caused by Injected Currents. *The Journal of Physiology*, *168*(4), 911–931. https://doi.org/10.1113/jphysiol.1963.sp007230

Grillner, S. (1981). Control of Locomotion in Bipeds, Tetrapods, and Fish. In *Comprehensive Physiology* (pp. 1179–1236). Wiley. https://doi.org/10.1002/cphy.cp010226

Grillner, S., & Jessell, T. M. (2009). Measured motion: searching for simplicity in spinal locomotor networks. *Current Opinion in Neurobiology*, *19*(6), 572–586. https://doi.org/10.1016/j.conb.2009.10.011

Grillner, S., McClean, A., Sigvardt, K., Wallen, P., & Wilen, M. (1981). Activation of NMDA-receptors elicits "Fictive locomotion" in lamprey spinal cord in vitro. *Acta Physiologica Scandinavica*, *113*(4), 549–551. https://doi.org/10.1111/j.1748-1716.1981.tb06937.x

Hägglund, M., Borgius, L., Dougherty, K. J., & Kiehn, O. (2010). Activation of groups of excitatory neurons in the mammalian spinal cord or hindbrain evokes locomotion. *Nature Neuroscience*, *13*(2), 246–252. https://doi.org/10.1038/nn.2482

Hamill, O. P., Marty, A., Neher, E., Sakmann, B., & Sigworth, F. J. (1981). Improved patch-clamp techniques for high-resolution current recording from cells and cell-free membrane patches. *Pflügers Archiv - European Journal of Physiology*, *391*(2), 85–100. https://doi.org/10.1007/BF00656997

Hayashi, M., Hinckley, C. A., Driscoll, S. P., Moore, N. J., Levine, A. J., Hilde, K. L., Sharma, K., & Pfaff, S. L. (2018). Graded Arrays of Spinal and Supraspinal V2a Interneuron Subtypes Underlie Forelimb and Hindlimb Motor Control. *Neuron*, *97*(4), 869-884.e5. https://doi.org/10.1016/j.neuron.2018.01.023

Hernandez, P., Elbert, K., & Droge, M. H. (1991). Spontaneous and NMDA evoked motor rhythms in the neonatal mouse spinal cord: an in vitro study with comparisons to in situ activity. *Experimental Brain Research*, *85*(1). https://doi.org/10.1007/BF00229987

Hinckley, C. A., Hartley, R., Wu, L., Todd, A., & Ziskind-Conhaim, L. (2005). Locomotor-Like Rhythms in a Genetically Distinct Cluster of Interneurons in the Mammalian Spinal Cord. *Journal of Neurophysiology*, *93*(3), 1439–1449. https://doi.org/10.1152/jn.00647.2004

Hinckley, C. A., Wiesner, E. P., Mentis, G. Z., Titus, D. J., & Ziskind-Conhaim, L. (2010). Sensory Modulation of Locomotor-Like Membrane Oscillations in Hb9-Expressing Interneurons. *Journal of Neurophysiology*, *103*(6), 3407–3423. https://doi.org/10.1152/jn.00996.2009

Hochman, S., Jordan, L. M., & MacDonald, J. F. (1994). N-methyl-D-aspartate receptor-mediated voltage oscillations in neurons surrounding the central canal in slices of rat spinal cord. *Journal of Neurophysiology*, *72*(2), 565–577. https://doi.org/10.1152/jn.1994.72.2.565

Hodgkin, A. L., & Huxley, A. F. (1952). A quantitative description of membrane current and its application to conduction and excitation in nerve. *The Journal of Physiology*, *117*(4), 500–544. https://doi.org/10.1113/jphysiol.1952.sp004764

Hultborn, H. (2006). Spinal reflexes, mechanisms and concepts: From Eccles to Lundberg and beyond. *Progress in Neurobiology*, *78*(3–5), 215–232. https://doi.org/10.1016/j.pneurobio.2006.04.001

Husch, A., Cramer, N., & Harris-Warrick, R. M. (2011). Long-duration perforated patch recordings from spinal interneurons of adult mice. *Journal of Neurophysiology*, *106*(5), 2783–2789. https://doi.org/10.1152/jn.00673.2011

Ijspeert, A. J. (2003). Locomotion, Vertebrate. *THe Handbook of Brain Theory and Neural Networks*.

Jankowska, E., Jukes, M. G. M., Lund, S., & Lundberg, A. (1967). The Effect of DOPA on the Spinal Cord 6. Half-centre organization of interneurones transmitting effects from the flexor reflex afferents. *Acta Physiologica Scandinavica*, *70*(3–4), 389–402. https://doi.org/10.1111/j.1748-1716.1967.tb03637.x

Jessell, T. M. (2000). Neuronal specification in the spinal cord: inductive signals and transcriptional codes. *Nature Reviews Genetics*, *1*(1), 20–29. https://doi.org/10.1038/35049541

Jiang, Z., Carlin, K. P., & Brownstone, R. M. (1999). An in vitro functionally mature mouse spinal cord preparation for the study of spinal motor networks. *Brain Research*, *816*(2), 493–499. https://doi.org/10.1016/S0006-8993(98)01199-8

Jordan, L. M. (1998). Initiation of Locomotion in Mammals. *Annals of the New York Academy of Sciences*, *860*(1), 83–93. https://doi.org/10.1111/j.1749-6632.1998.tb09040.x

Jordan, L. M., Liu, J., Hedlund, P. B., Akay, T., & Pearson, K. G. (2008). Descending command systems for the initiation of locomotion in mammals. *Brain Research Reviews*, *57*(1), 183–191. https://doi.org/10.1016/j.brainresrev.2007.07.019

Kiehn, O. (2006). Locomotor Circuits in the Mammalian Spinal Cord. *Annual Review of Neuroscience*, *29*(1), 279–306. https://doi.org/10.1146/annurev.neuro.29.051605.112910

Kiehn, O. (2016). Decoding the organization of spinal circuits that control locomotion. *Nature Reviews Neuroscience*, *17*(4), 224–238. https://doi.org/10.1038/nrn.2016.9

Kiehn, O., Hultborn, H., & Conway, B. A. (1992). Spinal locomotor activity in acutely spinalized cats induced by intrathecal application of noradrenaline. *Neuroscience Letters*, *143*(1–2), 243–246. https://doi.org/10.1016/0304-3940(92)90274-B

Kiehn, O., & Kjaerulff, O. (1996). Spatiotemporal characteristics of 5-HT and dopamine-induced rhythmic hindlimb activity in the in vitro neonatal rat. *Journal of Neurophysiology*, *75*(4), 1472–1482. https://doi.org/10.1152/jn.1996.75.4.1472

KIEHN, O., & KJAERULFF, O. (1998). Distribution of Central Pattern Generators for Rhythmic Motor Outputs in the Spinal Cord of Limbed Vertebrates a. *Annals of the New York Academy of Sciences*, *860*(1), 110–129. https://doi.org/10.1111/j.1749-6632.1998.tb09043.x

Kjaerulff, O., & Kiehn, O. (1996). Distribution of Networks Generating and Coordinating Locomotor Activity in the Neonatal Rat Spinal Cord *In Vitro* : A Lesion Study. *The Journal of Neuroscience*, *16*(18), 5777–5794. https://doi.org/10.1523/JNEUROSCI.16-18-05777.1996

Kremer, E., & Lev-Tov, A. (1997). Localization of the Spinal Network Associated With Generation of Hindlimb Locomotion in the Neonatal Rat and Organization of Its Transverse Coupling System. *Journal of Neurophysiology*, *77*(3), 1155–1170. https://doi.org/10.1152/jn.1997.77.3.1155

Kudo, N., & Yamada, T. (1987). locomotor activity in a spinal cord-indlimb muscles preparation of the newborn rat studied in vitro. *Neuroscience Letters*, *75*(1), 43–48. https://doi.org/10.1016/0304-3940(87)90072-3

Laliberte, A. M., Goltash, S., Lalonde, N. R., & Bui, T. V. (2019). Propriospinal Neurons: Essential Elements of Locomotor Control in the Intact and Possibly the Injured Spinal Cord. *Frontiers in Cellular Neuroscience*, *13*. https://doi.org/10.3389/fncel.2019.00512

Lanuza, G. M., Gosgnach, S., Pierani, A., Jessell, T. M., & Goulding, M. (2004). Genetic identification of spinal interneurons that coordinate left-right locomotor activity necessary

for walking movements. *Neuron*, *42*(3), 375–386. https://doi.org/10.1016/s0896-6273(04)00249-1

Lapointe, N. P., Rouleau, P., Ung, R., & Guertin, P. A. (2009). Specific role of dopamine D1 receptors in spinal network activation and rhythmic movement induction in vertebrates. *The Journal of Physiology*, *587*(7), 1499–1511. https://doi.org/10.1113/jphysiol.2008.166314

Lin, S., Hari, K., Black, S., Khatmi, A., Fouad, K., Gorassini, M. A., Li, Y., Lucas-Osma, A. M., Fenrich, K. K., & Bennett, D. J. (2023). Locomotor-related propriospinal V3 neurons produce primary afferent depolarization and modulate sensory transmission to motoneurons. *Journal of Neurophysiology*, *130*(4), 799–823. https://doi.org/10.1152/jn.00482.2022

Liu, J., & Jordan, L. M. (2005). Stimulation of the Parapyramidal Region of the Neonatal Rat Brain Stem Produces Locomotor-Like Activity Involving Spinal 5-HT 7 and 5-HT 2A Receptors. *Journal of Neurophysiology*, *94*(2), 1392–1404. https://doi.org/10.1152/jn.00136.2005

Lundberg, A. (1979). *Multisensory Control of Spinal Reflex Pathways* (pp. 11–28). https://doi.org/10.1016/S0079-6123(08)60803-1

MacLean, J. N., Schmidt, B. J., & Hochman, S. (1997). NMDA Receptor Activation Triggers Voltage Oscillations, Plateau Potentials and Burstinq in Neonatal Rat Lumbar Motoneurons *ln Vitro*. *European Journal of Neuroscience*, *9*(12), 2702–2711. https://doi.org/10.1111/j.1460-9568.1997.tb01699.x

McClellan, A. D., & Grillner, S. (1984). Activation of 'fictive swimming' by electrical microstimulation of brainstem locomotor regions in an in vitro preparation of the lamprey central nervous system. *Brain Research*, *300*(2), 357–361. https://doi.org/10.1016/0006-8993(84)90846-1

McCrea, D. A., & Rybak, I. A. (2008). Organization of mammalian locomotor rhythm and pattern generation. *Brain Research Reviews*, *57*(1), 134–146. https://doi.org/10.1016/j.brainresrev.2007.08.006

Menelaou, E., & McLean, D. L. (2019). Hierarchical control of locomotion by distinct types of spinal V2a interneurons in zebrafish. *Nature Communications*, *10*(1), 4197. https://doi.org/10.1038/s41467-019-12240-3

Nowak, L., Bregestovski, P., Ascher, P., Herbet, A., & Prochiantz, A. (1984). Magnesium gates glutamate-activated channels in mouse central neurones. *Nature*, *307*(5950), 462–465. https://doi.org/10.1038/307462a0

O'Donovan, M., & Landmesser, L. (1987). The development of hindlimb motor activity studied in the isolated spinal cord of the chick embryo. *The Journal of Neuroscience*, *7*(10), 3256–3264. https://doi.org/10.1523/JNEUROSCI.07-10-03256.1987

Perrier, J.-F., & Delgado-Lezama, R. (2005). Synaptic Release of Serotonin Induced by Stimulation of the Raphe Nucleus Promotes Plateau Potentials in Spinal Motoneurons of the Adult Turtle. *The Journal of Neuroscience*, *25*(35), 7993–7999. https://doi.org/10.1523/JNEUROSCI.1957-05.2005

Picciotto, M. R., & Wickman, K. (1998). Using Knockout and Transgenic Mice to Study Neurophysiology and Behavior. *Physiological Reviews*, *78*(4), 1131–1163. https://doi.org/10.1152/physrev.1998.78.4.1131

Poon, M. L. T. (1980). Induction of swimming in lamprey by L-DOPA and amino acids. *Journal of Comparative Physiology ? A*, *136*(4), 337–344. https://doi.org/10.1007/BF00657354

Raastad, M., Enríquez-Denton, M., & Kiehn, O. (1998). Synaptic signaling in an active central network only moderately changes passive membrane properties. *Proceedings of the*

*National Academy of Sciences*, *95*(17), 10251–10256. https://doi.org/10.1073/pnas.95.17.10251

Rancic, V., & Gosgnach, S. (2021). Recent Insights into the Rhythmogenic Core of the Locomotor CPG. *International Journal of Molecular Sciences*, *22*(3), 1394. https://doi.org/10.3390/ijms22031394

Roberts, A., Soffe, S. R., Wolf, E. S., Yoshida, M., & Zhao, F. -Y. (1998). Central Circuits Controlling Locomotion in Young Frog Tadpoles. *Annals of the New York Academy of Sciences*, *860*(1), 19–34. https://doi.org/10.1111/j.1749-6632.1998.tb09036.x

Rossignol, S., & Terjung, R. (1996). Neural Control of Stereotypic Limb Movements. In *Comprehensive Physiology* (pp. 173–216). Wiley. https://doi.org/10.1002/cphy.cp120105

Rybak, I. A., Dougherty, K. J., & Shevtsova, N. A. (2015). Organization of the Mammalian Locomotor CPG: Review of Computational Model and Circuit Architectures Based on Genetically Identified Spinal Interneurons. *Eneuro*, *2*(5), ENEURO.0069-15.2015. https://doi.org/10.1523/ENEURO.0069-15.2015

Rybak, I. A., Stecina, K., Shevtsova, N. A., & McCrea, D. A. (2006). Modelling spinal circuitry involved in locomotor pattern generation: insights from the effects of afferent stimulation. *The Journal of Physiology*, *577*(2), 641–658. https://doi.org/10.1113/jphysiol.2006.118711

Schmidt, B. J., & Jordan, L. M. (2000). The role of serotonin in reflex modulation and locomotor rhythm production in the mammalian spinal cord. *Brain Research Bulletin*, *53*(5), 689–710. https://doi.org/10.1016/S0361-9230(00)00402-0

Sengupta, M., & Bagnall, M. W. (2022). *V2b neurons act via multiple targets in spinal motor networks*. https://doi.org/10.1101/2022.08.01.502410

Sharples, S. A., Humphreys, J. M., Jensen, A. M., Dhoopar, S., Delaloye, N., Clemens, S., & Whelan, P. J. (2015). Dopaminergic modulation of locomotor network activity in the neonatal mouse spinal cord. *Journal of Neurophysiology*, *113*(7), 2500–2510. https://doi.org/10.1152/jn.00849.2014

Sherrington, C. S. (1910). Flexion-reflex of the limb, crossed extension-reflex, and reflex stepping and standing. *The Journal of Physiology*, *40*(1–2), 28–121. https://doi.org/10.1113/jphysiol.1910.sp001362

Shik, M. L., Severin, F. V, & Orlovskiĭ, G. N. (1966). Control of walking and running by means of electric stimulation of the midbrain. *Biofizika*, *11*(4), 659–666.

Smith, J. C., & Feldman, J. L. (1985). Motor patterns for respiration and locomotion generated by an in vitro brainstem-spinal cord from neonatal rat. *Society of Neuroscience*, *11*.

Smith, J. C., & Feldman, J. L. (1987). In vitro brainstem-spinal cord preparations for study of motor systems for mammalian respiration and locomotion. *Journal of Neuroscience Methods*, *21*(2–4), 321–333. https://doi.org/10.1016/0165-0270(87)90126-9

Smith, J. C., Feldman, J. L., & Schmidt, B. J. (1988). Neural mechanisms generating locomotion studied in mammalian brain stem-spinal cord in vitro. *The FASEB Journal*, *2*(7), 2283–2288. https://doi.org/10.1096/fasebj.2.7.2450802

Tao, Y., & Droge, M. H. (1992). Comparison of spontaneous motor pattern generation in non-hemisected and hemisected mouse spinal cord. *Neuroscience Letters*, *144*(1–2), 116–120. https://doi.org/10.1016/0304-3940(92)90729-Q

Viala, D., & Buser, P. (1974). Effects of a decarboxylase inhibitor on the Dopa and 5-HTP induced changes in the locomotor-like discharge pattern of rabbit hind limb nerves. *Psychopharmacologia*, *40*(3), 225–233. https://doi.org/10.1007/BF00429416

Wallen, P., & Grillner, S. (1987). N-methyl-D-aspartate receptor-induced, inherent oscillatory activity in neurons active during fictive locomotion in the lamprey. *The Journal of Neuroscience*, *7*(9), 2745–2755. https://doi.org/10.1523/JNEUROSCI.07-09-02745.1987

Wheatley, M., Edamura, M., & Stein, R. B. (1992). A comparison of intact and in-vitro locomotion in an adult amphibian. *Experimental Brain Research*, *88*(3). https://doi.org/10.1007/BF00228189

Whelan, P., Bonnot, A., & O'Donovan, M. J. (2000). Properties of Rhythmic Activity Generated by the Isolated Spinal Cord of the Neonatal Mouse. *Journal of Neurophysiology*, *84*(6), 2821–2833. https://doi.org/10.1152/jn.2000.84.6.2821

Wiggin, T. D., Montgomery, J. E., Brunick, A. J., Peck, J. H., & Masino, M. A. (2022). V3 Interneurons Are Active and Recruit Spinal Motor Neurons during *In Vivo* Fictive Swimming in Larval Zebrafish. *Eneuro*, *9*(2), ENEURO.0476-21.2022. https://doi.org/10.1523/ENEURO.0476-21.2022

Wilson, J. M., Robert Hartley, David J. Maxwell, Andrew J. Todd, Ivo Lieberam, Julia A. Kaltschmidt, Yutaka Yoshida, Thomas M. Jessel, & Robert M. Brownstone. (2005). Conditional Rhythmicity of Ventral Spinal Interneurons Defined by Expression of the Hb9 Homeodomain Protein. *Journal of Neuroscience*, *25*(24), 5710–5719. https://doi.org/10.1523/JNEUROSCI.0274-05.2005

Zagoraiou, L., Akay, T., Martin, J. F., Brownstone, R. M., Jessell, T. M., & Miles, G. B. (2009). A Cluster of Cholinergic Premotor Interneurons Modulates Mouse Locomotor Activity. *Neuron*, *64*(5), 645–662. https://doi.org/10.1016/j.neuron.2009.10.017

Zaman, M. M. (2024). *Effect of serotonin on ventral V3 populations* . University of Manitoba.

Zaporozhets, E., Cowley, K. C., & Schmidt, B. J. (2004). A reliable technique for the induction of locomotor-like activity in the in vitro neonatal rat spinal cord using brainstem electrical stimulation. *Journal of Neuroscience Methods*, *139*(1), 33–41. https://doi.org/10.1016/j.jneumeth.2004.04.009

Zelenin, P. V., Vemula, M. G., Lyalka, V. F., Kiehn, O., Talpalar, A. E., & Deliagina, T. G. (2021). Differential Contribution of V0 Interneurons to Execution of Rhythmic and Nonrhythmic Motor Behaviors. *The Journal of Neuroscience*, *41*(15), 3432–3445. https://doi.org/10.1523/JNEUROSCI.1979-20.2021

Zhang, H., Deska-Gauthier, D., MacKay, C. S., Hari, K., Lucas-Osma, A. M., Borowska-Fielding, J., Letawsky, R. L., Rancic, V., Akay, T., Fenrich, K. K., Bennett, D. J., & Zhang, Y. (2025). Widespread innervation of motoneurons by spinal V3 neurons globally amplifies locomotor output in mice. *Cell Reports*, *44*(1), 115212. https://doi.org/10.1016/j.celrep.2024.115212

Zhang, H., Shevtsova, N. A., Deska-Gauthier, D., Mackay, C., Dougherty, K. J., Danner, S. M., Zhang, Y., & Rybak, I. A. (2022). The role of V3 neurons in speed-dependent interlimb coordination during locomotion in mice. *ELife*, *11*. https://doi.org/10.7554/eLife.73424

Zhang, J., Lanuza, G. M., Britz, O., Wang, Z., Siembab, V. C., Zhang, Y., Velasquez, T., Alvarez, F. J., Frank, E., & Goulding, M. (2014). V1 and V2b Interneurons Secure the Alternating Flexor-Extensor Motor Activity Mice Require for Limbed Locomotion. *Neuron*, *82*(1), 138–150. https://doi.org/10.1016/j.neuron.2014.02.013

Zhang, Narayan, S., Geiman, E., Lanuza, G. M., Velasquez, T., Shanks, B., Akay, T., Dyck, J., Pearson, K., Gosgnach, S., Fan, C.-M., & Goulding, M. (2008). V3 Spinal Neurons Establish a Robust and Balanced Locomotor Rhythm during Walking. *Neuron*, *60*(1), 84–96. https://doi.org/10.1016/j.neuron.2008.09.027

Zhong, G., Diaz-Rios, M., & Harris-Warrick, R. M. (2006). Intrinsic and Functional Differences among Commissural Interneurons during Fictive Locomotion and Serotonergic Modulation in the Neonatal Mouse. *Journal of Neuroscience*, *26*(24), 6509–6517. https://doi.org/10.1523/JNEUROSCI.1410-06.2006

Zhong, G., Droho, S., Crone, S. A., Dietz, S., Kwan, A. C., Webb, W. W., Sharma, K., & Harris-Warrick, R. M. (2010). Electrophysiological Characterization of V2a Interneurons and Their Locomotor-Related Activity in the Neonatal Mouse Spinal Cord. *The Journal of Neuroscience*, *30*(1), 170–182. https://doi.org/10.1523/JNEUROSCI.4849-09.2010